Resilience to health shocks and the spatial extent of local labour markets: evidence from the COVID-19 outbreak in Italy

Mattia Borsati[a,d,*], Michele Cascarano[b], Marco Percoco[a]

[a] *Dept. of Social and Political Sciences and GREEN, Bocconi University, Milan, Italy*
[b] *Economic Research Unit, Bank of Italy, Trento, Italy*
[d] *Present affiliation: Department of Econometrics, Statistics and Applied Economics, University of Barcelona*

Abstract

In addition to the general issue that fewer interpersonal contacts reduce the speed of contagion, less attention has been paid to the spatial configuration of such contacts. In Italy, COVID-19 severely affected the most industrialized area of the country, where the network of commuting flows is particularly dense. We investigate the relationship between workers' mobility and the diffusion of the disease by computing, for each municipality, the intensive and extensive margins of commuting flows and by measuring excess mortality over the period of January-May 2020. We find that, if commuting patterns were 90% of the ones observed in the data, Italy would have suffered approximately 2 300 fewer fatalities during the first pandemic cycle.

Keywords: COVID-19, Resilience, Local labour market, Commuting flows, Mobility

JEL Classification Numbers: H12, I18, J61, R41

Introduction

The daily mobility of individuals for motives of labour is one of the main features of developed societies, so the spatial extent of local labour markets is in fact defined on the basis of the geography of commuting flows. The openness of such areas generates costs and benefits for the governance of the local economy, particularly in the case of a pandemic, as it is one of the conditions that determine their ability to contain such an intense health disaster (Gong et al., 2020). In this article, we investigate how the openness of local labour markets, as defined by the structure of the commuting network, influences the resilience of cities to health shocks, such as the COVID-19 outbreak. In particular, we explore the aforementioned dynamics in Italy, the first Western country to be deeply affected by the disease.

There are several reasons why we believe that such an empirical analysis is needed for a thorough comprehension of the phenomenon. First, the initial burst of the virus spread across

*Corresponding author.
Email addresses: mattia.borsati@unibocconi.it (Mattia Borsati), michele.cascarano@bancaditalia.it (Michele Cascarano), marco.percoco@unibocconi.it (Marco Percoco)

Italy first and foremost in the most industrialized area of the country, suggesting a correlation between the structural features of local economies and the epidemic. Second, places characterized by high density of economic activities also exhibit dense networks of spatial interactions (especially in the form of commuting flows), and these flows in their turn place such places at more severe epidemiological risk, as shown by past (Charu et al., 2017; Zhou et al., 2019) and present (Fang et al., 2020; Glaeser et al., 2020) epidemics. In fact, Bergamo, the city among the provincial capitals with the largest share of incoming and outgoing workers compared to the population overall, is the one that also experienced the greatest increase in fatalities recorded in March 2020 (+429%), compared to the 2015-2019 average. Not surprisingly, the openness of Bergamo's labour market is remarkable because it is the epicentre of the largest industrial district in the whole nation[1]

In response to the diffusion of COVID-19 during the first months of 2020, several national governments imposed unprecedented lockdown restrictions to slow the infection rate and save lives. Indeed, in the absence of medical treatments, such as vaccines or pharmaceuticals, the limitation of interpersonal contacts was the key policy for containing viral infections (Haushofer and Metcalf, 2020; Van Bavel et al., 2020). As a result, the travel behaviours of people have been drastically altered (De Vos, 2020), with dramatic economic and social consequences (Bonaccorsi et al., 2020).

Although the literature exploring the main drivers of the geographical diffusion of COVID-19 is sizeable, understanding how local economies are related to the perturbation caused by the pandemic is still an open research question. In this article, we contribute to this ongoing debate by investigating the role played by the spatial extent of local labour markets in filtering the initial spread of the disease through workers mobility and, therefore, in influencing the resilience of cities to the health shock.

To this end, we analyse the pre-existing characteristics of commuting patterns at the municipality level[2] using data from the latest official country-wide assessment of mobility for Italy. Similarly, we measure the local depth of the pandemic shock by considering excess mortality over the period of January-May 2020, comprising several weeks both before and after the most critical part of the first pandemic cycle. We also consider a broad set of additional municipality characteristics to control for other specific dynamics. After assembling the novel dataset, our empirical strategy exploits within-municipality variation in excess mortality over time by estimating a two-way fixed effects model in which all of our explanatory variables are interacted with month dummies.

Our article provides some relevant novelties in two directions: first, we examine the structure of the commuting network by computing both the intensive and extensive margins of commuting flows; and second, we exploit more granular and heterogeneous data by performing the analysis at the municipality level, while most of the previous studies focused on main cities, provinces, or regions.

More precisely, we compute two synthetic indices that describe commuting flows under different perspectives: the intensity of external mobility and the centrality of each municipality.

The first index - the intensive margin - is defined as the total number of workers moving from and to a municipality over its population, similar to what is proposed by Murgante et al. (2020). In other words, it is a proxy for the share of the population exposed to the possibility of the virus being imported from elsewhere. The second index - the extensive margin - is based on the topological concept of relative degree centrality of a node within a network, measuring the importance and the openness of a municipality, as defined by Patuelli et al. (2009, 2010). In other words, the aim is to measure the number of other different places (each of which may have a different infection rate) to which the municipality is connected.

In addition, we further investigate the commuting dynamics by exploring the spatial heterogeneity of lockdown intensities induced by different government policies, such as the anticipation of mobility restrictions (imposed using containment areas) and the reduction of active workers (imposed using the closure of non-essential economic activities). Shedding light on whether such measures played a role in flattening the mortality curve is therefore important in the design of future policies aimed at containing new outbreaks.

Our findings suggest that the spatial extent of local labour markets was crucial in influencing the resilience of cities to the COVID-19 health shock. In particular, a 1 percentage point increase in the intensive margin is associated, on average, with 1.43 and 0.91 percentage point increases in excess mortality in March and April 2020, respectively, while the same increase in the extensive margin is associated with a 3.44 increase in our outcome of interest in April. As a result, more isolated and less central places are found to be more resilient than others. Moreover, we report suggestive evidence on the role of containment areas and businesses closure in reducing COVID-19-related fatalities - and therefore in increasing the resilience of local economies - by cutting down mobility among municipalities.

Within the massive empirical literature on COVID-19, our research is mainly related to two separate lines of work that have proposed commuting flows and the characteristics of local economies as major explanations for the observed unequal spread of COVID-19 across sub-national areas. By focusing on those contributions dealing with the Italian context[3], a first strand of research has shown that human mobility played a crucial role in the propagation of the disease during the first wave of the pandemic, as highlighted by the striking relationship between mobility flows and both the net reproduction number (R_t) of the virus (Cintia et al., 2020) and the resulting excess mortality (Ascani et al., 2021b; Iacus et al., 2020). Linked to this line of work, a group of studies have analysed the mobility patterns of people during the emergency and the consequent change in the structure of commuting flows, including Beria and Lunkar (2021) and Pepe et al. (2020). A second strand of research has emphasized how the most industrialized area of the country was more severely affected by the earliest phase of the pandemic due to its socioeconomic characteristics, such as greater domestic and international connectivity (Bourdin et al., 2021), and a greater degree of interaction between workers employed in locations endowed with a high density of industries (Ascani et al., 2021a). Hence, more productive and interconnected areas were found to be more exposed to the spread of infectious diseases than others (Bloise and Tancioni, 2021).

Within the broad literature on regional resilience, our research is also related to a rich amount of studies that have analysed how the social, demographic, and economic characteristics of territories determine their heterogeneous resilience to a particular shock, including (among others) Bristow and Healy (2014); Diodato and Weterings (2015); Kitsos and Bishop (2018), and Martin et al. (2016).

In this article, we connect these three strands of research by investigating the interplay between labour market dynamics, the initial spread of COVID-19, and the resilience to the shock.

The remainder of the article is organized as follows. First, we provide a conceptual framework to the notion of resilience in times of a pandemic and we briefly summarize the timeline of the COVID-19 crisis in Italy. Second, we describe the data used in the analysis. Third, we discuss the empirical strategy, our main results, and the robustness checks. Finally, we explore the spatial heterogeneity of lockdown intensities and we conclude the study.

The anatomy of resilience shaped by COVID-19

Resilience in a time of pandemic

In the current COVID-19 crisis, the notion of resilience has increasingly taken up not only within academic research, but also within institutional and policy debates. Such multidisciplinary concept does not have a unique definition, as its meaning varies according to the purposes for which it is used and depends on the scale, nature, and duration of the shock to which it refers (Martin, 2018). Broadly speaking, it defines the ability of a system to absorb an external shock, bounce back, and reorganize itself afterwards. Such concept has been progressively introduced into the regional economic research when a proliferation of studies started to tackle the question of why some local economies where more resilient than others in facing an increasing number of shocks and disruptions, such as natural hazards (e.g., Hong et al., 2021; Zhou et al., 2010) and financial crisis (e.g., Capello et al., 2015; Davies, 2011).

Following the conceptual framework developed by Martin and Sunley (2015) and Martin et al. (2016), the resilience of a local system is usually defined as a complex process involving several phases, such as i) the vulnerability to a shock (defined as the propensity to be hit by that shock), ii) the resistance to it (measured as the impact of the shock on a specific outcome), iii) the reorientation after the shock (defined as the ability to adjust and adapt to the shock), and iv) the recoverability from the shock (measured by the speed of return to a previous equilibrium). According to the same framework, these phases are influenced by many factors, such as local economic characteristics and any supportive policy aimed at softening the impact of the shock (see Figure 1 for a detailed explanation of each phase of the resilience process).

[Figure 1 about here.]

Compared to the other shocks to which the literature on regional resilience normally refers to, the specific features of the disruption caused by COVID-19 are of a different nature, so

that their analysis has given rise to new research questions (Gong et al., 2020). For instance, understanding why some places were more severely affected than others during the first wave of the pandemic is still a relatively unexplored issue. Given that infectious diseases tend to spread through human interaction, the risk for a local economy of being hit by a health shock strongly depends on its openness, which is shaped by the daily mobility of individuals for motives of labour. Therefore, the analysis of the geography of commuting flows is crucial when it comes to understanding the vulnerability phase (Massaro et al., 2018). Furthermore, these flows affect a type of resistance called "human" resistance (Ascani et al., 2021b), which can be measured as excess mortality compared to a previous average. In its turn, such an unfortunate outcome directly affects the "economic" resistance of a local system because it determines the introduction of lockdown restrictions (aimed at slowing down the infection rate) on which the reorientation and recoverability phases crucially depend.

Since our period of analysis covers a period in which the health crisis has always been far from over, this article focuses on the first two phases of the resilience process (i.e., those included in the area bounded by the dotted line in Figure 1). On this basis, we investigate the extent to which the pre-existing commuting network - shaped by the structural features of local economies - affected excess mortality during the first pandemic cycle in Italy. Although partial, this analysis may represents a first assessment of the resilience of cities to the COVID-19 health shock.

COVID-19 in Italy

Our empirical analysis focuses on Italy, the first Western country that was forced to shut down its economy to "flatten the curve" and contain the diffusion of COVID-19. Therefore, Italy represents the ideal scenario for investigating the relationship between commuting flows and the initial diffusion of the virus because government and citizens were unprepared to face the pandemic, while both policymakers and populations of other European countries have been influenced by the Italian case. Such an unfortunate situation limits the number of confounding factors because there were no countermeasures or policy responses during the first weeks of the outbreak.

The timeline of the main events that occurred during the first wave of the pandemic (summarised in Figure 2) is the following. The first two COVID-19 cases in Italy were officially detected on January 30, after a Chinese couple travelled from Wuhan to Milan, Verona, Parma, and Florence. The first cases of secondary transmission were identified near Codogno and Vo' (two municipalities in the Lombardy and Veneto regions, respectively) on February 21, and two days later, the Italian government enforced mobility restrictions into and from these areas (DPCM1, 2020). On March 4, all schools and universities were closed (DPCM2, 2020). On March 8, the lockdown was imposed for the first relevant "red zone" of the country (DPCM3, 2020), that is, the whole Lombardy region and 14 additional provinces within the Emilia-Romagna, Marche, Piedmont, and Veneto regions[4] (see Figure 7 for a detailed map). On March 11, the lockdown was extended to the whole nation (DPCM4, 2020), and many business activities open to the

public were forced to close. Between March 22 and March 25, the "economic" lockdown was tightened further by shutting down all non-essential economic activities and prohibiting any movement of people on Italian soil with few exceptions, such as for work or health reasons (DPCM5, 2020; DPCM6, 2020). This step marked the so called "phase 1" of the epidemic, which gradually ended between May 4 and May 18.

[Figure 2 about here.]

Data

To study the spatial diffusion of the recent COVID-19 pandemic, we rely on two main data sources: the *Italian National Institute of Statistics* (ISTAT) and the *Italian Institute for Environmental Protection and Research* (ISPRA). In the following section we describe the variables used in the empirical analysis.

Measuring resilience through excess mortality

For 7 357 Italian municipalities out of 7 904 (covering approximately 95% of the total population), we obtain data released by ISTAT on July 9, 2020, that is, the monthly number of fatalities occurring during the first five months of 2020 and the average monthly number of fatalities occurring during the same period in 2015-2019. For the sake of simplicity, we refer to the latter data as the "baseline" throughout the rest of the article. Then, our outcome of interest is *mortality_growth*, defined as the increase in fatalities recorded in January, February, March, April and May 2020 compared to the same period in the "baseline"[5]:

$$mortality\_growth_{it} = \frac{fatalities_{it}^{2020} - fatalities_{it}^{baseline}}{fatalities_{it}^{baseline}} \quad (1)$$

where i and t denote the municipality and the month, respectively. This measure of the incidence of COVID-19 is directly related to the notion of local resilience (Boschma, 2015) since it computes the burden of the disease as a deviation from a pre-existing trend. We consider excess mortality our main outcome of interest over the official number of COVID-19 cases because it allows us to overcome, at least partially, major measurement errors and endogeneity issues related to the number of reported cases, such as non-random differences in screening procedures and testing capacity among areas. Indeed, it allows us to observe any COVID-19-related fatalities, even before February 21, when the first Italian COVID-19 hotspots were identified[6]. Similarly, we prefer total fatalities over official COVID-19 fatalities because the latter are no longer considered a reliable measure due to differences in classification among hospitals (Buonanno et al., 2020). Moreover, it is plausible to expect that the official numbers are underestimating the true increase in mortality since a substantial number of people died without being tested (Ciminelli and Garcia-Mandicó, 2020; Bartoszek et al., 2020). Indeed, during the first quarter of 2020, Italy experienced 46 909 more deaths with respect to the average number of

fatalities occurring in the same period during 2015-2019, while the official COVID-19 fatalities declared by the Department of Civil Protection numbered 27 938 (INPS, 2020). Hence, it is likely that the majority of the remaining 18 971 fatalities were also caused by the pandemic[7]. In addition, the use of such measures also allows us to consider the indirect effects of the pandemic, such as the possible increase in fatalities caused by other diseases that were not treated as usual due to hospital congestion.

Measuring the spatial extent of local labour markets

The aim of this article is to investigate the role played by the spatial extent of local labour markets in influencing their resilience to the spread of COVID-19. To this end, we use data on the network of commuting flows reported in the 2011 census in the form of a nationwide origin-destination matrix. We measure the intensity of external mobility of each municipality by considering both the out-flows, indicating the total number of workers w_{ij} moving from their residential municipality i to any other municipality $j = 1 \dots n$ (excluding j = i), and the in-flows, indicating the total number of workers w_{ji} moving to municipality i from any other municipality j. We compute, for each municipality, the intensive margin of commuting, defined as the sum of the incoming and outgoing flows over the 2011 population of the area:

$$intensive\_margin_i = \frac{\sum_{j=1}^{n}(w_{ij} + w_{ji})}{population_i} \tag{2}$$

We also consider a topological index. We first compute the total number of direct outward and inward connections of each municipality (*degree_centrality*), that is, the set of origin-destination routes used by at least one worker to commute. Then, we define the extensive margin of commuting as the ratio between the observed and the maximum possible number of connections $(n-1)$ of a municipality:

$$extensive\_margin_i = \frac{degree\_centrality_i}{n-1} \tag{3}$$

Control variables

To separate the effect of commuting flows from other confounding factors, we consider another important dimension linked to the movement of people, such as internal mobility. To this end - and by relying on the same 2011 census - we compute an *internal_mobility* index as the ratio of self-flows, indicating the total number of workers w_{ii} moving within their residential municipality i to reach the workplace, to the 2011 population of the area.

Then, we further control for other variables potentially correlated with both excess mortality and commuting patterns. In particular, we add all those predictors that are essential in standard epidemiological models to explain the spatial diffusion of a disease (e.g., Bisin and Moro, 2020). Given that living in urban areas and in close proximity is likely to increase the probability of infection (Armillei et al., 2021; Desmet and Wacziarg, 2021), we first capture relevant geographic

and demographic characteristics by including two dummy variables that take the value of 1 if a municipality is located near the sea (*coastal*) or at medium-high altitude (*mountainous*) and 0 otherwise, the log of the population density (*ln_density*), and a proxy of physical proximity, defined as the log of the average number of square metres per inhabitant in occupied dwellings (*ln_house_m²_pc*).

Second, given that the fatality rates for males are two to three times higher than for females (Porcheddu et al., 2020), that the fatality rate is positively correlated with a larger presence of elderly people (Knittel and Ozaltun, 2020), that nursing homes and hospitals were the locations of the first outbreaks of the pandemic (Barnett and Grabowski, 2020), and that pollution can be an important co-determinant of COVID-19-related fatalities in northern Italy[8] (Coker et al., 2020; Conticini et al., 2020; Dettori et al., 2021), we also control for five measures of vulnerability to the pandemic: the share of male population at the municipality level (*share_males*), the share of population older than 75 years old at the municipality level (*share_over75*), the share of individuals older than 65 years old cohabiting with younger individuals at the municipality level (*share_cohab_over65*), the number of hospital beds per inhabitant at the province level (*hospital_beds_pc*), and the PM10, defined as the average values of $\mu g/m^3$ at the province level (*pm10*).

Third, we account for differences in economic structure between areas by including a dummy variable that takes the value of 1 if a municipality is located within an industrial district (*district*) and 0 otherwise. Indeed, recent literature shows how thicker local labour markets (characterized by high density of industries) may foster higher levels of business and social interactions (e.g., Ascani et al., 2021b). Finally, we have seen how the pandemic has induced many workers to perform their duties from home, preventing them from traveling. Thus, it might be that municipalities with larger numbers of "remote" workers experienced fewer COVID-19-related fatalities with respect to others. To capture this possible dynamic, we compute a working remotely index (*remote_working*) by weighting the set of working remotely indices provided by Barbieri et al. (2021) by the labour force composition of each municipality (as defined by the 1-digit ATECO[9] sections).

All of the data are publicly available[10]. Table A.1 reports standard descriptive statistics of the variables used in the empirical analysis, Table A.2 summarizes their definition (as well as their reference year, the unit of observation, and the data source), while Figure B.2 reports a correlation matrix among covariates.

Descriptive evidence

In this section we briefly describe the spatial patterns of our main variables of interest. Figure 3 plots the spatial evolution of *mortality_growth* in March 2020, i.e., when Italy was severely affected by the pandemic (see Figure B.3 for the same map in the other months). Clearly, we can note how COVID-19-related fatalities appear to be spatially clustered in the northern part of Italy, particularly in the Lombardy region and across the Po Valley area[11]. Overall, the virus

spread first and foremost in the most industrialized area of the country, suggesting a possible correlation between the structural features of local economies, such as the spatial interactions of workers, and the epidemic. As we can see in Figures 4 and 5, this area also shows high density of commuting flows, both in the intensive and the extensive components (see Figure B.4 for additional maps of other control variables). The visual correlation, especially between excess mortality and the intensity of external mobility, is striking and suggests a specific role of commuting flows in placing more connected places at more severe epidemiological risks.

[Figure 3 about here.]

[Figure 4 about here.]

[Figure 5 about here.]

Empirical analysis

Econometric model

To examine the relationship between the characteristics of commuting flows and excess mortality, we estimate the following equation:

$$\begin{aligned} mortality\_growth_{it} = \beta_0 + \beta_t intensive\_margin_i \times \delta_t + \gamma_t extensive\_margin_i \times \delta_t \\ + \eta_t Z_i \times \delta_t + \alpha_i + \delta_t + \epsilon_{it} \end{aligned} \tag{4}$$

where $mortality\_growth_{it}$ measures the increase in fatalities occurring in municipality i in month t, compared to the same period at "baseline". On the right-hand side, $intensive\_margin_i$ and $extensive\_margin_i$ are our municipality commuting indices interacted with a vector of monthly specific fixed effects, δ_t, accounting for the nationwide common evolution of excess mortality in a given month, such as the seasonal trend. By excluding January as the pre-outbreak period, the vectors of coefficients β_t and γ_t capture the impact of the structural characteristics of commuting flows on excess mortality over the various months of the pandemic cycle. $Z_i \times \delta_t$ indicates the internal mobility, geographic, demographic, vulnerability, and economic controls, also interacted with month dummies. Then, α_i is a full set of municipality-level fixed effects intended to absorb any difference in excess mortality due to time-invariant characteristics. Hence, by controlling for all of these observed and unobserved characteristics, our identifying assumption is that no other factor correlated with workers commuting systematically affects excess mortality. Finally, given that the geography of commuting flows analysed in this article essentially describes the spatial extent of local labour markets (Kropp and Schwengler, 2016), ϵ_{it} are heteroskedasticity- and autocorrelation-consistent standard errors, respectively clustered at the local labour market (LLM) level.

Estimation results

Tables 1 and 2 report regression results for Equation 4. The rationale for the structure of the two tables (which can be read sequentially) is to progressively include fixed effects and control variables to test the strength of our estimates.

In Table 1, the first two columns report the estimated coefficients for the specifications in which the intensive and extensive margins, interacted with month dummies, are included one at a time. Accordingly, the main effects of the interactions are included as well. In column 3, the two margins are simultaneously estimated, while in column 4, the specification adds a full set of region fixed effects because the Italian national health system is managed at the regional level. Finally, column 5 substitutes the region fixed effects with a full set of municipality fixed effects to better control for time-invariant characteristics of each observation potentially correlated with both excess mortality and commuting flows[12]. Overall, almost all of the estimated coefficients of the two margins preserve their signs and significance throughout the columns, their magnitudes decreasing as the specifications become less parsimonious.

[Table 1 about here.]

In Table 2 we report estimates of regressions in which we have extended the set of controls. Interestingly, the estimated coefficients of the two margins remain consistent as, moving from the most parsimonious specification in column 1 to the most extended in column 4, their magnitude decreases without leading to a substantial increase in the standard error. Thus, our estimates suggest an important role played by the spatial extent of local labour markets in influencing the resilience of municipalities during the COVID-19 outbreak. Indeed, the intensity of external mobility - the intensive margin - and the topological centrality of a municipality - the extensive margin - are positively correlated with excess mortality during the most critical part of the pandemic. This empirical evidence suggests how greater connectivity renders places less resilient to epidemic health shocks.

[Table 2 about here.]

For simplicity, we discuss further only the estimates in column 4 because they are obtained with the most complete specification in relation to our data. Given that January is our reference period, regression results are close to zero and not statistically significant in February, that is, when the COVID-19 virus had just begun to spread. As expected, the *intensive_margin* shows its strongest correlation with excess mortality in March, when Italy was suddenly and severely affected by the pandemic. The coefficient indicates that, holding constant the other variables, a 1 percentage point increase in the share of population moving from and to a municipality is associated, on average, with a 1.43 percentage point increase in excess mortality. Then, following the introduction of all of the containment measures previously described, this positive correlation remain significant in April but with a smaller magnitude (0.91), while it loses significance and approaches zero in May, hinting how the lockdown was crucial in reducing excess mortality by

cutting down workers mobility among municipalities. The *extensive_margin*, instead, shows its statistically significant correlation only in April, likely because the most central nodes of the commuting network played a pivotal role in spreading the disease later. The coefficient indicates that a 1 percentage point increase in the ratio between the observed and the maximum possible number of connections of a municipality is associated, on average, with a 3.44 percentage point increase in our outcome of interest, all else being equal[13].

That said, we provide some back-of-the-envelope calculations by considering three scenarios in which the intensive margins among Italian municipalities would be equal to 90%, 80%, and 70% of those actually observed in our data. In other words, we are interested in understanding what the reduction in *mortality_growth* would have been had commuting flows been lower. For each scenario, Figure 6 shows these median reductions for the months in which our *intensive_margin* coefficients are strongly significant. By focusing on the mildest scenario[14], where our commuting index is cut by 10%, 4.8% and 5.3% median reductions in mortality growth on March and April would translates into 1 346 and 997 lives saved[15] across Italy, respectively.

[Figure 6 about here.]

Robustness checks

In the following section we briefly describe a set of robustness checks aimed at corroborating our empirical findings. First, the *intensive_margin*, which is defined as the sum of incoming and outgoing flows over the population of the area, could have some "extreme" values. Indeed, as shown in Figure 4, for 58 of 7 345 municipalities, the value of this index is greater than 1, implying that the number of workers moving from and to the municipality is greater than the number of residents. To check that these possible outliers are not affecting our results, we winsorize the *intensive_margin* by setting all of the data greater than the 99$^{\text{th}}$ percentile to the 99$^{\text{th}}$ percentile and all of the data less than the 1$^{\text{st}}$ percentile to the 1$^{\text{st}}$ percentile. By so doing, we obtain an index that takes values between 0 and 1. Accordingly, we also winsorize in the same way the *extensive_margin*. Then, we estimate the most complete specification of Equation 4 with these new variables. As shown in column 1 of Table 3, the regression results are very consistent with the main ones provided in Table 2, indicating that these possible outliers are not driving our estimates.

Second, the first wave of COVID-19 has spread dramatically in some regions and not in others. The reasons for this phenomenon are difficult to assess since they most likely depend on many factors that favour the spread of the disease through different channels. For instance, in Italy, the virus severely affected the most industrialized regions, such as Lombardy, Emilia-Romagna, Piedmont, and Veneto, which differ from the rest of the country in several characteristics. Thus, it might be relevant to verify that our previous findings are not affected by such differences among areas. To this end, we estimate the most complete specification of Equation 4 with a more "balanced" sample by considering only the municipalities located within these

four regions. The regression results provided in column 2 of Table 3 suggest that the intensity of external mobility remains a determining factor in spread of the disease in the northern regions, while there is no evidence that the topology of the network contributed as well. Our interpretation is that, within the most infected areas of the country, what matters most is the total number of workers moving between municipalities, rather than the number of different connections.

Third, despite 9-year lagged explanatory variables perhaps solving some endogeneity issues, a reasonable concern is whether the 2011 commuting flows remain informative about the current ones. As proved by Gatto et al. (2020), they are since the spatial patterns of work-related mobility seem to be remarkably preserved over such a long time interval. Moreover, we further test the consistency over time of the commuting network by comparing the 2011 share of outgoing flows, indicating the total number of workers moving from a municipality over its population, with the 2019 ones[16]. As shown by the regression line depicted in Figure B.6, we find an almost one-to-one association between the two shares ($R^2 = 0.95$). Finally, we computed the intensive and extensive margins using the 2001 and 1991 official country-wide assessments of mobility for Italy. If our 2011 mobility patterns are truly "structural", we should expect similar estimates by relying on the 2001 and 1991 data. Once again, we estimate the most complete specification of Equation 4, and the related regression results are provided in columns 3 and 4 of Table 3. The estimated coefficients involving the intensive margin are consistent in sign, significance, and magnitude with the main ones provided by Table 2 (lending additional reliability to our empirical findings), while the estimated coefficient involving the extensive margin in April is barely not statistically significant using the 2001 data.

[Table 3 about here.]

Spatial heterogeneity implied by lockdown intensities

In this section, we provide some further evidence for the relationship between the spatial extent of local labour markets and the initial diffusion of the virus by exploring the spatial heterogeneity of lockdown intensities induced by two policy interventions. The first source of geographical heterogeneity is based on some municipalities being located within the first relevant "red zone" of the country, which was enforced on March 8 (DPCM3, 2020). In this area, mobility restrictions were anticipated compared to the rest of Italy; hence, it is plausible to expect that this early reduction in workers commuting played a role in flattening the mortality curve more rapidly inside the "red zone" than outside[17]. The second source of geographical heterogeneity is based on the "economic" lockdown imposed between March 22 and March 25 (DPCM5, 2020; DPCM6, 2020), which forced the closure of non-essential economic activities, as well as those with high indices of physical proximity (Barbieri et al., 2021), indicating that the different sectoral composition of economic activities among municipalities leads to different shares of inactive workers, which consequently translate into different reductions in commuting flows between areas.

The introduction of the "red zone"

We start our analysis by first considering the heterogeneity imposed by the introduction of a containment area, such as the "red zone". To this end, we first set a dummy variable (*red_zone*) equal to 1 if a municipality is located within the locked area, the boundaries of which are drawn in Figure 7.

[Figure 7 about here.]

Then, we estimate the following augmented version of Equation 4:

$$\begin{aligned} mortality\_growth_{it} = \beta_0 &+ \theta_t intensive\_margin_i \times red\_zone_i \times \delta_t \\ &+ \omega_t extensive\_margin_i \times red\_zone_i \times \delta_t \\ &+ \beta_t intensive\_margin_i \times \delta_t + \gamma_t extensive\_margin_i \times \delta_t \\ &+ \psi_t red\_zone_i \times \delta_t + \eta_t Z_i \times \delta_t + \alpha_i + \delta_t + \epsilon_{it} \end{aligned} \tag{5}$$

where we add the triple interactions among; i) the intensive and extensive margins; ii) the *red_zone* dummy; and iii) the set of month dummies. Accordingly, the area main effects are also included.

Table 4 reports regression results for Equation 5. Similar to Table 2, all of the specifications include month and municipality fixed effects, while columns 1-4 progressively add our sets of control variables. We focus on the coefficients estimated by the most complete specification in column 4. Given that the "red zone" was enforced on March 8, that the incubation time of the disease can be approximated in approximately 5 days (Lauer et al., 2020), and that reported COVID-19 fatalities tend to occur around 18-21 days after infection (Yang et al., 2020), we should observe an impact of the anticipated mobility restrictions in the area in reducing mortality from April onwards. As expected, the coefficients associated with the triple interactions involving the intensive margin in April and May are negative, but only the latter is statistically significant. This outcome suggests how an early reduction in the intensity of commuting flows, induced by an anticipated lockdown, could foster - after some weeks - a faster reduction in excess mortality related to external mobility, compared to areas without restrictions. Thus, containment areas could be useful to increase the resilience of local economies. Here, the triple interactions involving the extensive margin are not at all significant, likely because of collinearity with the *red_zone* dummy, which captures most of the variability, as shown in Figure 5[18]. Finally, we clearly find a positive and consequently decreasing correlation between being located within the "red zone" and excess mortality. This finding confirms that the boundaries of the containment area were based on the high infection rate of the municipalities within it.

[Table 4 about here.]

The introduction of the "economic" lockdown

We now turn to exploiting the variation in the share of inactive workers due to the closure of non-essential economic activities. To this end, we rely on the most recent official data provided by ISTAT[19] to compute the number of active and inactive workers for each municipality, which are based on the list of ATECO sectors not suspended by the Italian government during the first part of 2020 (see Table A.4 for a detailed list of sectors that were allowed to operate). Then, we compute our share of interest by simply dividing the number of inactive workers by the total number of workers in the area:

$$share\_inactive_i = \frac{inactive\_w_i}{w_i} \tag{6}$$

At this point, we are interested in understanding how much this "economic" lockdown has tightened commuting flows among municipalities, given that many workers no longer had to reach their workplaces. To do so, we compute the share of inactive commuters for each municipality in the following way:

$$share\_inactive\_commuters_i = \frac{\sum_{j=1}^{n}(w_{ij} \times share\_inactive_j + w_{ji} \times share\_inactive_i)}{\sum_{j=1}^{n}(w_{ij} + w_{ji})} \tag{7}$$

where the total number of workers moving from and to a municipality (as explained in Equation 2) has been first multiplied by the share of inactive workers in the municipality of destination and then weighted by the total incoming and outgoing flows. Next, we define municipalities with the largest share of inactive commuters by setting a dummy variable (*high_inactive*) that equals 1 if the value computed through Equation 7 is greater than the 66^{th} percentile. These municipalities - visually correlated with the most industrialized regions of the country - are plotted in Figure 8.

[Figure 8 about here.]

To test whether the closure of non-essential economic activities played a role in reducing COVID-19-related fatalities by tightening commuting flows further, we estimate the following augmented version of Equation 4:

$$\begin{aligned} mortality\_growth_{it} = \beta_0 &+ \theta_t intensive\_margin_i \times high\_inactive_i \times \delta_t \\ &+ \beta_t intensive\_margin_i \times \delta_t + \gamma_t extensive\_margin_i \times \delta_t \\ &+ \psi_t high\_inactive_i \times \delta_t + \eta_t Z_i \times \delta_t + \alpha_i + \delta_t + \epsilon_{it} \end{aligned} \tag{8}$$

where we add the triple interaction among: i) the intensive margin; ii) the *high_inactive* dummy; and iii) the set of month dummies. Accordingly, the area main effects are included. Note that we do not add the triple interaction involving the extensive margin because the closure

of non-essential economic activities affected the intensity of commuting flows, rather than the number of connections between municipalities.

Table 5 reports regression results for Equation 8. Different from the previous tables, column 1 directly reports the estimated coefficients for the most complete specification. Here, the negative and significant coefficient associated with the triple interaction in April suggests that municipalities with the largest share of inactive commuters would benefit from a faster reduction in excess mortality. Interestingly, this finding is in line with the recent empirical evidence provided by Borri et al. (2020) and Di Porto et al. (2020). In columns 2 and 3, we further examined this point by splitting the sample between municipalities located inside and outside the "red zone". The rationale for the sample split is testing whether this second policy made an additional contribution to reducing COVID-19-related fatalities - through a further restriction of workers commuting - even within an area that had already been affected by the first policy. As it is plausible to expect, the effectiveness of the "economic" lockdown in reducing commuting flows further (and therefore in better controlling virus transmissions) lessened within the "red zone". In fact, the coefficients associated with the triple interactions are nowhere significant in column 2. Conversely, the coefficients retain their magnitudes and significance in column 3, indicating that the national dynamics also hold outside the "red zone". Accordingly, the same explanation applies.

[Table 5 about here.]

Conclusions

The diffusion of COVID-19 is imposing tremendous challenges on our society, and it seems that now, more than in the past few decades, geography is considered a crucial feature for resilience to such a shock. With reference to the Italian case, the virus spread first and foremost in the most industrialized area of the country, where the high density of economic activities also exhibits dense networks of commuting flows. To the best of our knowledge, this article is among the very few exploring the role played by the openness of local labour markets, as defined by the structure of the commuting network, in filtering the initial spread of the virus and, therefore, in influencing the resilience of Italian municipalities to the health shock. To this end, we computed the intensive and extensive margins of commuting flows, and we measured the spread of COVID-19 by considering excess mortality over the first five months of 2020, with clear implications in terms of measurement of resilience.

Using a rich and novel dataset, we have found that, during the most critical part of the first pandemic cycle (i.e., March and April 2020), municipalities with larger shares of population commuting from and to their borders for motives of labour tended to have higher COVID-19-related fatalities. Moreover, our findings also indicate that it is not only the intensity of external mobility that can influence the speed of diffusion of the virus and the depth of the shock but also the centrality of each municipality within a network of commuting flows. Indeed, municipalities

strongly connected to many other different places experienced higher excess mortality in April as well. A back-of-the-envelope calculation suggests that, if structural commuting patterns were 90% of the ones observed in the data, Italy would have suffered 1 346 and 997 fewer fatalities in March and April 2020, respectively. Finally, we explored the spatial heterogeneity of lockdown intensities induced by different government policies, such as the introduction of the first relevant "red zone" of the country and the closure of non-essential economic activities. We report suggestive evidence on the role of these policies in favouring a faster reduction in excess mortality and, therefore, in increasing the resilience of local economies.

The overall conclusion arising from our analysis is that places more isolated and less central are found to be more resilient than others, all else being equal. This finding, in its turn, suggests policy actions to strengthen the resistance to the shock - and overcome the epidemic - considering not only the intensity of commuting flows but also addressing specific hotspots, central in the network of commuting flows.

Acknowledgements

We are very grateful for comments and suggestions that substantially improved the paper by the Editor and three anonymous Referees. We also thank Antonio Accetturo, Domenico Depalo, members of the Department of Econometrics, Statistics and Applied Economics (Public Policy) of the University of Barcelona, as well as participants at the SIET 2020, 2020 annual meeting of the territorial research network of the Bank of Italy, ITEA 2021, and ERSA 2021. The views expressed in this article are those of the authors and do not necessarily correspond with those of their institutions. We have no conflicts of interest to disclose.

Notes

[1]Industrial districts are "self-contained" labour markets mainly consisting of small- and medium-sized enterprises specializing in the same economic activity. According to the latest industry and services national census, the industrial district of Bergamo is the largest in terms of population (802 731) and embedded municipalities (123).

[2]To avoid misunderstandings, we understand the openness of local labour markets by means of commuting flows at the municipality level. This choice is driven by the need to exploit excess mortality data as granular as possible. Therefore, our empirical analysis does not use the official definition of local labour market (as defined by the Italian National Institute of Statistics) as the unit of observation.

[3]For the sake of conciseness, this unavoidably incomplete literature review focuses only on those contributions that have used the Italian scenario as their case study.

[4]The 14 additional provinces that completed the containment areas are Modena, Parma, Piacenza, Reggio nell'Emilia, Rimini, Pesaro e Urbino, Alessandria, Asti, Novara, Verbano-Cusio-Ossola, Vercelli, Padova, Treviso, and Venezia.

[5]The evolution of excess mortality in Italy during the period of analysis is plotted in Figure B.1. We acknowledge an anonymous Referee for pointing out the existence of alternative estimates of excess mortality for Italy, such as the one provided by Cerqua et al. (2021) using machine learning techniques. Unfortunately, we are not able to fit our model specification (which is based on monthly data) with estimates computed over different time intervals.

[6]By analysing the first three complete genomes of SARS-CoV-2, Zehender et al. (2020) showed that the virus was present in Italy weeks before the first reported case.

[7]During the period of May 25-July 15 2020, the Italian Ministry of Health and ISTAT conducted an epidemiological investigation to estimate the percentage of the population that likely contracted the infection by sampling 150 000 individuals throughout the whole Italian territory. The results (based on 64 660 serological tests) show that the number of people who contracted the virus is equal to 2.5% of the population and therefore 6 times more than the official COVID-19 cases detected over the pandemic cycle (ISTAT, 2020).

[8]Several studies in the medical literature have shown that individuals living in highly polluted areas have a reduced capacity to react to respiratory diseases and pneumonias (Pope III and Dockery, 2006).

[9]The ATECO 2007 classification is the Italian equivalent of the European NACE Rev. 2 classification.

[10]*mortality_growth* data are retrieved from `https://www.istat.it/it/archivio/240401`. *intensive_margin*, *extensive_margin*, and *internal_mobility* data are retrieved from `https://www.istat.it/it/archivio/157423`. *coastal*, *mountainous*, and *ln_density* data are retrieved from `https://www.istat.it/it/archivio/156224`. *ln_house_m*^{2}*_pc*, *share_over*75, and *share_cohab_over*65 data are retrieved from `http://ottomilacensus.istat.it/`. *share_males* and *hospital_beds_pc* data are retrieved from `http://dati.istat.it/`. *pm*10 data are retrieved from `https://www.isprambiente.gov.it/it/pubblicazioni/stato-dellambiente`. *district* data are retrieved from `https://www.istat.it/it/archivio/150320`. *remote_working* data are retrieved from `http://dati-censimentoindustriaeservizi.istat.it/Index.aspx` and Barbieri et al. (2021).

[11]Nevertheless, by relying on a spatial weights matrix constructed through Euclidean distances without neighbourless municipalities, the Moran's I index for spatial autocorrelation of our outcome of interest is relatively low (0.13).

[12]Given that our *intensive_margin* and *extensive_margin* are time-invariant variables, they are omitted from column 5 because of collinearity with municipality fixed effects.

[13]For the sake of completeness, estimates of all of the control variables (supported by a brief discussion) are reported in Table A.3, while Figure B.5 plots the coefficients of the most complete specification of Table 2 with their 95% and 99% confidence intervals.

[14]By way of example, this scenario would correspond to the situation in which the city of Bergamo, the provincial capital with both the highest *intensive_margin* and *mortality_growth* in March (as discussed in the introductory section, would have commuting flows comparable to the provincial capital of Monza.

[15] With reference to our 7 357 municipalities, the average number of fatalities occurring in Italy at the "baseline" were 55 065 in March and 49 144 in April, while the total number of fatalities occurring during the same months in the 2020 were 82 867 (+50.5%) and 67 805 (+38.0%), respectively. According to the reductions in mortality growth for these months computed by our back-of-the-envelope calculations, the mildest scenario would have led to *mortality_growth* of 48.0% (50.5%-(50.5%*4.8%)) in March and 35.9% (38.0%-(38.0%*5.3%) in April. Hence, the "counterfactual" number of fatalities during the most critical part of the pandemic cycle would have been 81 521 in March and 66 808 in April.

[16] Although a more up to date origin-destination matrix would undoubtedly be preferred, it is not available. At the municipality level, the most recent data on commuting (retrieved from `http://dati-censimentipermanenti.istat.it/Index.aspx`) provide information only on the aggregate 2019 out-flows.

[17] Caselli et al. (2020), providing empirical evidence that this containment area significantly lowered individual mobility.

[18] For the same reason, the estimated coefficients of the extensive margin interacted with month dummies are not directly interpretable.

[19] Data are retrieved from `https://www.istat.it/it/archivio/241341`. For the sake of clarity, ISTAT data (which are based on the 2017 *Frame Territoriale* register) focus on workers in the industrial and service sectors. Workers employed in other economic activities, such as agriculture and public administration, are excluded from the registry because these sectors are outside the scope of business statistics.

References

Armillei, F., Filippucci, F., Fletcher, T., 2021. Did Covid-19 hit harder in peripheral areas? The case of Italian municipalities. Economics & Human Biology , 101018.

Ascani, A., Faggian, A., Montresor, S., 2021a. The geography of COVID-19 and the structure of local economies: The case of Italy. Journal of Regional Science 61, 407–441.

Ascani, A., Faggian, A., Montresor, S., Palma, A., 2021b. Mobility in times of pandemics: evidence on the spread of Covid-19 in Italy's labour market areas. Structural Change and Economic Dynamics 58, 444–454.

Barbieri, T., Basso, G., Scicchitano, S., 2021. Italian workers at risk during the Covid-19 epidemic. Italian Economic Journal , 1–21.

Barnett, M.L., Grabowski, D.C., 2020. Nursing homes are ground zero for COVID-19 pandemic, in: JAMA Health Forum, American Medical Association. pp. e200369–e200369.

Bartoszek, K., Guidotti, E., Iacus, S.M., Okrój, M., 2020. Are official confirmed cases and fatalities counts good enough to study the COVID-19 pandemic dynamics? A critical assessment through the case of Italy. Nonlinear Dynamics 101, 1951–1979.

Beria, P., Lunkar, V., 2021. Presence and mobility of the population during the first wave of Covid-19 outbreak and lockdown in Italy. Sustainable Cities and Society 65, 102616.

Bisin, A., Moro, A., 2020. Learning Epidemiology by Doing: The Empirical Implications of a Spatial-SIR Model with Behavioral Responses. NBER Working Paper No. 27590 .

Bloise, F., Tancioni, M., 2021. Predicting the spread of COVID-19 in Italy using machine learning: Do socio-economic factors matter? Structural Change and Economic Dynamics 56, 310–329.

Bonaccorsi, G., Pierri, F., Cinelli, M., Flori, A., Galeazzi, A., Porcelli, F., Schmidt, A.L., Valensise, C.M., Scala, A., Quattrociocchi, W., Pammolli, F., 2020. Economic and social consequences of human mobility restrictions under COVID-19. Proceedings of the National Academy of Sciences 117, 15530–15535.

Borri, N., Drago, F., Santantonio, C., Sobbrio, F., 2020. The "Great Lockdown": Inactive workers and mortality by Covid-19. CESifo Working Paper No. 8584 .

Boschma, R., 2015. Towards an evolutionary perspective on regional resilience. Regional Studies 49, 733–751.

Bourdin, S., Jeanne, L., Nadou, F., Noiret, G., 2021. Does lockdown work? A spatial analysis of the spread and concentration of Covid-19 in Italy. Regional Studies , 1–12.

Bristow, G., Healy, A., 2014. Regional Resilience: An Agency Perspective. Regional Studies 48, 923–935.

Buonanno, P., Galletta, S., Puca, M., 2020. Estimating the severity of Covid-19: evidence from the Italian epicenter. Plos one 15, e0239569.

Capello, R., Caragliu, A., Fratesi, U., 2015. Spatial heterogeneity in the costs of the economic crisis in Europe: are cities sources of regional resilience? Journal of Economic Geography 15, 951–972.

Caselli, M., Fracasso, A., Scicchitano, S., 2020. From the lockdown to the new normal: An analysis of the limitations to individual mobility in Italy following the Covid-19 crisis. GLO Discussion Paper No. 683 .

Cerqua, A., Di Stefano, R., Letta, M., Miccoli, S., 2021. Local mortality estimates during the COVID-19 pandemic in Italy. Journal of Population Economics , 1–29.

Charu, V., Zeger, S., Gog, J., Bjørnstad, O.N., Kissler, S., Simonsen, L., Grenfell, B.T., Viboud, C., 2017. Human mobility and the spatial transmission of influenza in the united states. PLoS computational biology 13, e1005382.

Ciminelli, G., Garcia-Mandicó, S., 2020. Covid-19 in Italy: An analysis of death registry data. Journal of Public Health 42, 723–730.

Cintia, P., Fadda, D., Giannotti, F., Pappalardo, L., Rossetti, G., Pedreschi, D., Rinzivillo, S., Bonato, P., Fabbri, F., Penone, F., et al., 2020. The relationship between human mobility and viral transmissibility during the COVID-19 epidemics in Italy. arXiv:2006.03141 .

Coker, E.S., Cavalli, L., Fabrizi, E., Guastella, G., Lippo, E., Parisi, M.L., Pontarollo, N., Rizzati, M., Varacca, A., Vergalli, S., 2020. The Effects of Air Pollution on COVID-19 Related Mortality in Northern Italy. Environmental and Resource Economics 76, 611–634.

Conticini, E., Frediani, B., Caro, D., 2020. Can atmospheric pollution be considered a co-factor in extremely high level of SARS-CoV-2 lethality in Northern Italy? Environmental pollution 261, 114465.

Davies, S., 2011. Regional resilience in the 2008–2010 downturn: comparative evidence from european countries. Cambridge Journal of Regions, Economy and Society 4, 369–382.

De Vos, J., 2020. The effect of COVID-19 and subsequent social distancing on travel behavior. Transportation Research Interdisciplinary Perspectives 5, 100121.

Desmet, K., Wacziarg, R., 2021. Understanding Spatial Variation in COVID-19 across the United States. Journal of urban economics , 103332.

Dettori, M., Deiana, G., Balletto, G., Borruso, G., Murgante, B., Arghittu, A., Azara, A., Castiglia, P., 2021. Air pollutants and risk of death due to COVID-19 in Italy. Environmental Research 192, 110459.

Di Porto, E., Naticchioni, P., Scrutinio, V., 2020. Partial lockdown and the spread of Covid-19: Lessons from the Italian case. CSEF Working Paper No. 569 .

Diodato, D., Weterings, A.B., 2015. The resilience of regional labour markets to economic shocks: Exploring the role of interactions among firms and workers. Journal of Economic Geography 15, 723–742.

DPCM1, 2020. Decreto del presidente del consiglio dei ministri 23 febbraio 2020 (in Italian). Retrieved 25 June 2020 from https://www.gazzettaufficiale.it/eli/id/2020/02/23/20A01228/sg.

DPCM2, 2020. Decreto del presidente del consiglio dei ministri 4 marzo 2020 (in Italian). Retrieved 25 June 2020 from https://www.gazzettaufficiale.it/eli/id/2020/03/04/20A01475/sg.

DPCM3, 2020. Decreto del presidente del consiglio dei ministri 8 marzo 2020 (in Italian). Retrieved 25 June 2020 from https://www.gazzettaufficiale.it/eli/id/2020/03/08/20A01522/sg.

DPCM4, 2020. Decreto del presidente del consiglio dei ministri 11 marzo 2020 (in Italian). Retrieved 25 June 2020 from https://www.gazzettaufficiale.it/eli/id/2020/03/11/20A01605/sg.

DPCM5, 2020. Decreto del presidente del consiglio dei ministri 22 marzo 2020 (in Italian). Retrieved 25 June 2020 from https://www.gazzettaufficiale.it/eli/id/2020/03/22/20A01807/sg.

DPCM6, 2020. Decreto del presidente del consiglio dei ministri 25 marzo 2020 (in Italian). Retrieved 25 June 2020 from https://www.gazzettaufficiale.it/eli/id/2020/03/26/20A01877/sg.

Fang, H., Wang, L., Yang, Y., 2020. Human mobility restrictions and the spread of the novel coronavirus (2019-nCoV) in China. Journal of Public Economics 191, 104272.

Gatto, M., Bertuzzo, E., Mari, L., Miccoli, S., Carraro, L., Casagrandi, R., Rinaldo, A., 2020. Spread and dynamics of the COVID-19 epidemic in Italy: Effects of emergency containment measures. Proceedings of the National Academy of Sciences 117, 10484–10491.

Glaeser, E.L., Gorback, C., Redding, S.J., 2020. Jue insight: How much does covid-19 increase with mobility? Evidence from New York and four other US cities. Journal of urban economics , 103292.

Gong, H., Hassink, R., Tan, J., Huang, D., 2020. Regional resilience in times of a pandemic crisis: The case of Covid-19 in China. Tijdschrift voor economische en sociale geografie 111, 497–512.

Haushofer, J., Metcalf, C.J.E., 2020. Which interventions work best in a pandemic? Science 368, 1063–1065.

Hong, B., Bonczak, B.J., Gupta, A., Kontokosta, C.E., 2021. Measuring inequality in community resilience to natural disasters using large-scale mobility data. Nature communications 12, 1–9.

Iacus, S.M., Santamaria, C., Sermi, F., Spyratos, S., Tarchi, D., Vespe, M., 2020. How human mobility explains the initial spread of Covid-19. Publications Office of the European Union .

INPS, 2020. Analisi della mortalità nel periodo di epidemia da covid-19 (in Italian). Retrieved 15 June 2020 from https://www.inps.it/docallegatiNP/Mig/Dati_analisi_bilanci/Nota_CGSA_mortal_Covid19_def.pdf.

ISTAT, 2020. Primi risultati dell'indagine di sieroprevalenza sul sars-cov-2 (in Italian). Retrieved 15 June 2020 from https://www.istat.it/it/files//2020/08/ReportPrimiRisultatiIndagineSiero.pdf.

Kitsos, A., Bishop, P., 2018. Economic resilience in Great Britain: the crisis impact and its determining factors for local authority districts. The Annals of Regional Science 60, 329–347.

Knittel, C.R., Ozaltun, B., 2020. What does and does not correlate with COVID-19 death rates. NBER Working Paper No. 27391 .

Kropp, P., Schwengler, B., 2016. Three-step method for delineating functional labour market regions. Regional Studies 50, 429–445.

Lauer, S.A., Grantz, K.H., Bi, Q., Jones, F.K., Zheng, Q., Meredith, H.R., Azman, A.S., Reich, N.G., Lessler, J., 2020. The incubation period of coronavirus disease 2019 (COVID-19) from publicly reported confirmed cases: estimation and application. Annals of internal medicine 172, 577–582.

Martin, R., Sunley, P., 2015. On the notion of regional economic resilience: conceptualization and explanation. Journal of Economic Geography 15, 1–42.

Martin, R., Sunley, P., Gardiner, B., Tyler, P., 2016. How regions react to recessions: Resilience and the role of economic structure. Regional Studies 50, 561–585.

Martin, R.L., 2018. Shocking aspects of regional development: Towards an economic geography of resilience, in: The new Oxford handbook of economic geography, pp. 839–864.

Massaro, E., Ganin, A., Perra, N., Linkov, I., Vespignani, A., 2018. Resilience management during large-scale epidemic outbreaks. Scientific reports 8, 1–9.

Murgante, B., Borruso, G., Balletto, G., Castiglia, P., Dettori, M., 2020. Why Italy First? Health, Geographical and Planning aspects of the Covid-19 outbreak. Sustainability 12, 5064.

Patuelli, R., Reggiani, A., Nijkamp, P., Bade, F.J., 2009. Spatial and commuting networks, in: Complexity and spatial networks. Springer, pp. 257–271.

Patuelli, R., Reggiani, A., Nijkamp, P., Bade, F.J., 2010. The evolution of the commuting network in Germany: Spatial and connectivity patterns. Journal of Transport and Land Use 2, 5–37.

Pepe, E., Bajardi, P., Gauvin, L., Privitera, F., Lake, B., Cattuto, C., Tizzoni, M., 2020. Covid-19 outbreak response, a dataset to assess mobility changes in Italy following national lockdown. Scientific data 7, 1–7.

Pope III, C.A., Dockery, D.W., 2006. Health effects of fine particulate air pollution: lines that connect. Journal of the air & waste management association 56, 709–742.

Porcheddu, R., Serra, C., Kelvin, D., Kelvin, N., Rubino, S., 2020. Similarity in case fatality rates (CFR) of COVID-19/SARS-COV-2 in Italy and China. The Journal of Infection in Developing Countries 14, 125–128.

Van Bavel, J.J., Baicker, K., Boggio, P.S., Capraro, V., Cichocka, A., Cikara, M., Crockett, M.J., Crum, A.J., Douglas, K.M., Druckman, J.N., et al., 2020. Using social and behavioural science to support COVID-19 pandemic response. Nature Human Behaviour 4, 460–471.

Yang, X., Yu, Y., Xu, J., Shu, H., Liu, H., Wu, Y., Zhang, L., Yu, Z., Fang, M., Yu, T., et al., 2020. Clinical course and outcomes of critically ill patients with SARS-CoV-2 pneumonia in Wuhan, China: a single-centered, retrospective, observational study. The Lancet Respiratory Medicine 8, 475–481.

Zehender, G., Lai, A., Bergna, A., Meroni, L., Riva, A., Balotta, C., Tarkowski, M., Gabrieli, A., Bernacchia, D., Rusconi, S., et al., 2020. Genomic characterization and phylogenetic analysis of SARS-COV-2 in Italy. Journal of Medical Virology 92, 1637–1640.

Zhou, H., Wang, J., Wan, J., Jia, H., 2010. Resilience to natural hazards: a geographic perspective. Natural hazards 53, 21–41.

Zhou, S., Zhou, S., Liu, L., Zhang, M., Kang, M., Xiao, J., Song, T., 2019. Examining the effect of the environment and commuting flow from/to epidemic areas on the spread of Dengue Fever. International Journal of Environmental Research and Public Health 16, 5013.

List of Figures

Figure 1: Process of local resilience

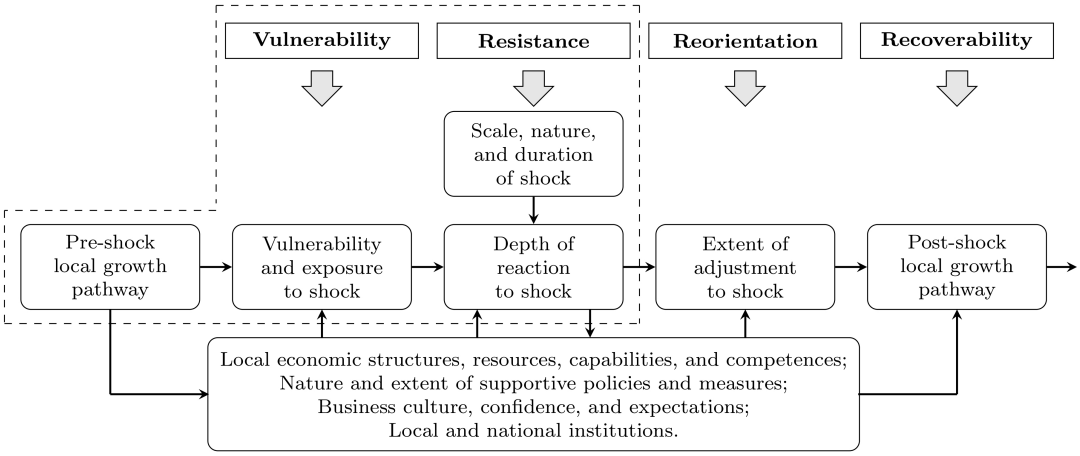

Source: Adapted from Martin and Sunley (2015) and Martin et al. (2016).

Figure 2: Timeline of the main events

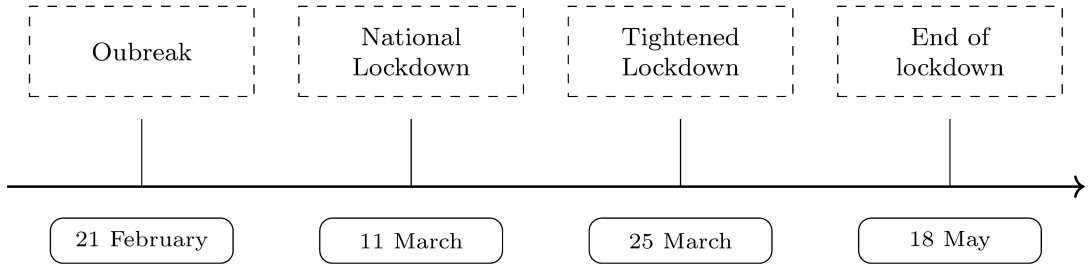

Notes: The figure shows the timeline of the main events that occurred in Italy during the first wave of the pandemic; hence, dates refer to the 2020. *Source*: Authors' own elaboration.

Figure 3: *mortality_growth* in March 2020, by municipality

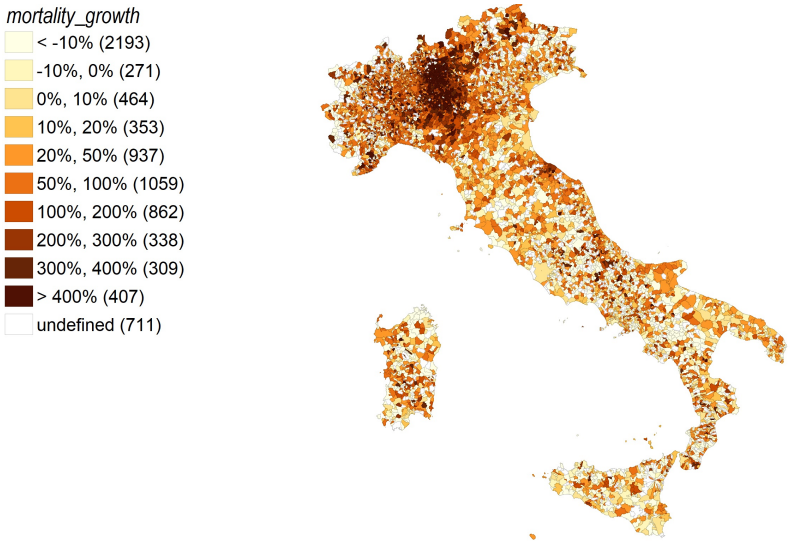

Source: Authors' own elaboration.

Figure 4: *intensive_margin*, by municipality

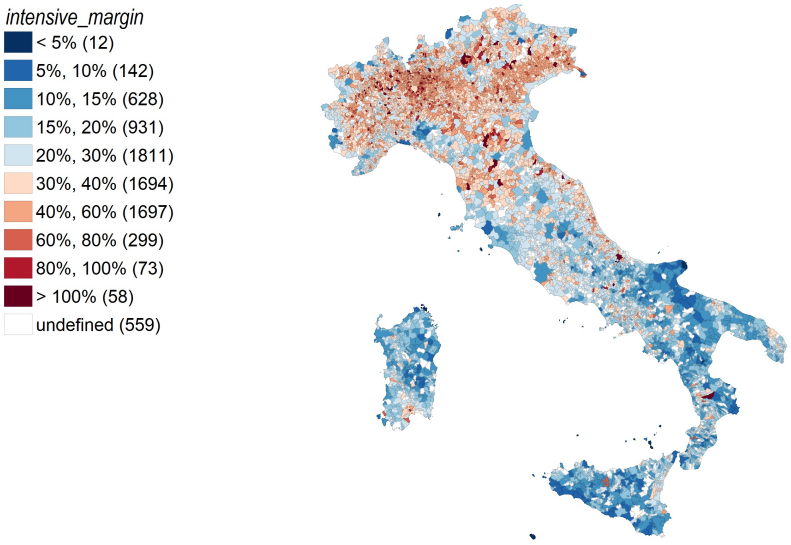

Source: Authors' own elaboration.

Figure 5: *extensive_margin*, by municipality

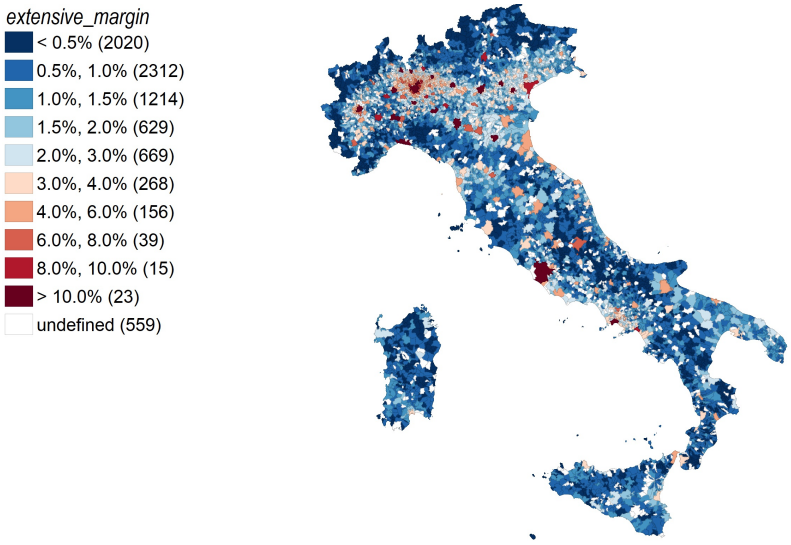

Source: Authors' own elaboration.

Figure 6: Reduction in *mortality_growth*, by month and scenario

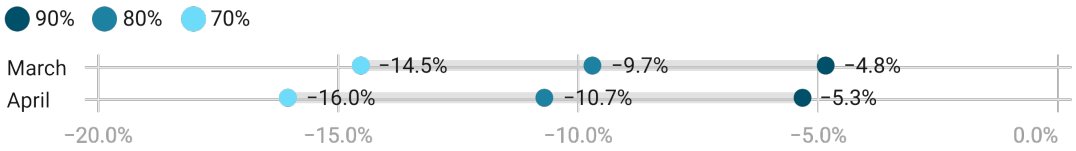

Notes: Estimates are based on back-of-the-envelope calculations along three scenarios in which the intensive margins would be equal to 90%, 80%, and 70% of those really observed in our data.

Figure 7: *red_zone* enforced on March 8, 2020

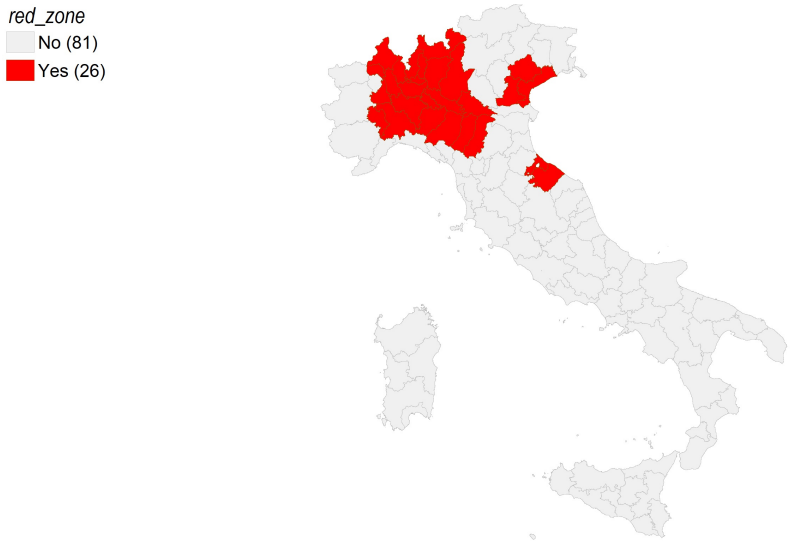

Source: Authors' own elaboration.

Figure 8: *share_inactive_commuters*, by municipality

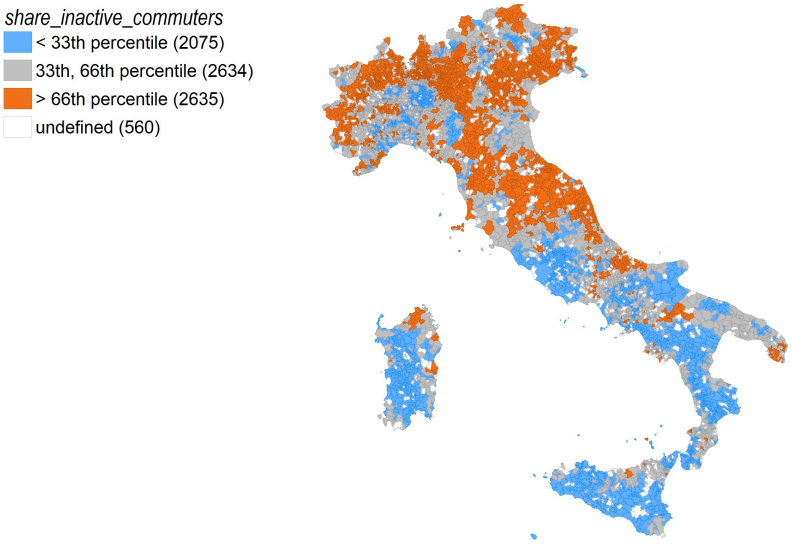

Source: Authors' own elaboration.

List of Tables

Table 1: Commuting indices and mortality growth (part 1)

	mortality_growth				
	(1)	(2)	(3)	(4)	(5)
intensive_margin × *February*	0.024		0.054	0.067	0.078
	(0.085)		(0.089)	(0.088)	(0.090)
intensive_margin × *March*	2.326***		2.053***	2.050***	2.070***
	(0.442)		(0.342)	(0.342)	(0.341)
intensive_margin × *April*	1.304***		1.178***	1.175***	1.191***
	(0.148)		(0.156)	(0.155)	(0.158)
intensive_margin × *May*	0.137		0.133	0.128	0.157*
	(0.085)		(0.088)	(0.088)	(0.089)
extensive_margin × *February*		-1.122	-1.365*	-1.475*	-1.424*
		(0.806)	(0.824)	(0.820)	(0.826)
extensive_margin × *March*		21.020**	11.770*	11.760	11.750
		(8.515)	(7.141)	(7.142)	(7.150)
extensive_margin × *April*		10.720***	5.434***	5.446***	5.380***
		(1.713)	(1.497)	(1.500)	(1.484)
extensive_margin × *May*		0.779	0.183	0.141	0.146
		(0.878)	(0.885)	(0.885)	(0.879)
intensive_margin	0.055		0.074	-0.441***	
	(0.049)		(0.051)	(0.081)	
extensive_margin		-0.519	-0.854	-5.551***	
		(0.579)	(0.583)	(1.238)	
constant	-0.052**	-0.027	-0.048**	0.143***	-0.033
	(0.022)	(0.018)	(0.023)	(0.045)	(0.025)
Month FE	✓	✓	✓	✓	✓
Region FE				✓	
Municipality FE					✓
Observations	35 916	35 916	35 916	35 916	35 916
R^2	0.07	0.06	0.07	0.10	0.08

Notes: All of the specifications present OLS estimates and include month, region, and municipality fixed effects as indicated. Standard errors clustered at the LLM level appear in parentheses. Significance values: ***p<0.01, **p<0.05, *p<0.10.

Table 2: Commuting indices and mortality growth (part 2)

	mortality_growth			
	(1)	(2)	(3)	(4)
$intensive\_margin \times February$	0.114	0.120	0.096	0.098
	(0.095)	(0.102)	(0.103)	(0.108)
$intensive\_margin \times March$	1.896***	1.804***	1.430***	1.427***
	(0.299)	(0.292)	(0.285)	(0.277)
$intensive\_margin \times April$	1.141***	1.034***	0.882***	0.906***
	(0.170)	(0.173)	(0.166)	(0.162)
$intensive\_margin \times May$	0.153	0.107	0.095	0.095
	(0.094)	(0.099)	(0.104)	(0.108)
$extensive\_margin \times February$	-1.881**	-0.698	-0.748	-0.771
	(0.891)	(1.075)	(1.086)	(1.093)
$extensive\_margin \times March$	14.000	11.820	6.064	8.556
	(8.531)	(7.995)	(6.930)	(6.596)
$extensive\_margin \times April$	6.032***	6.263***	2.643*	3.442**
	(1.767)	(1.680)	(1.567)	(1.590)
$extensive\_margin \times May$	0.198	-0.405	-1.352	-1.620
	(0.926)	(1.026)	(1.054)	(1.109)
constant	-0.034	-0.034	-0.034	-0.033
	(0.025)	(0.025)	(0.024)	(0.024)
Month FE	✓	✓	✓	✓
Municipality FE	✓	✓	✓	✓
Internal mobility $\times \delta_t$	✓	✓	✓	✓
Geographic controls $\times \delta_t$		✓	✓	✓
Demographic controls $\times \delta_t$		✓	✓	✓
Vulnerability controls $\times \delta_t$			✓	✓
Economic controls $\times \delta_t$				✓
Observations	35 916	35 916	35 916	35 916
R^2	0.08	0.09	0.10	0.11

Notes: All of the specifications present OLS estimates and include month and municipality fixed effects. Standard errors clustered at the LLM level appear in parentheses. Significance values: ***p<0.01, **p<0.05, *p<0.10.

Table 3: Commuting indices and mortality growth (robustness checks)

	mortality_growth			
	Winsorized	Subsample	2001 data	1991 data
	(1)	(2)	(3)	(4)
intensive_margin × *February*	0.203	0.084	0.082	0.024
	(0.144)	(0.127)	(0.106)	(0.114)
intensive_margin × *March*	1.940***	0.994**	1.488***	1.587***
	(0.353)	(0.419)	(0.327)	(0.391)
intensive_margin × *April*	1.317***	0.525**	0.880***	0.736***
	(0.200)	(0.219)	(0.168)	(0.175)
intensive_margin × *May*	0.210	-0.043	0.062	0.002
	(0.150)	(0.130)	(0.108)	(0.115)
extensive_margin × *February*	-1.690	-0.932	-0.499	-0.974
	(1.979)	(1.292)	(1.455)	(1.801)
extensive_margin × *March*	15.900	4.008	6.405	6.335
	(11.090)	(5.971)	(8.032)	(9.622)
extensive_margin × *April*	5.368*	-0.722	3.130	0.125
	(2.775)	(2.129)	(1.948)	(2.695)
extensive_margin × *May*	-2.993	-0.254	-1.788	-2.961
	(1.999)	(1.526)	(1.394)	(1.935)
constant	-0.033	-0.045	-0.034	-0.034
	(0.023)	(0.044)	(0.024)	(0.024)
Month FE	✓	✓	✓	✓
Municipality FE	✓	✓	✓	✓
Internal mobility × δ_t	✓	✓	✓	✓
Geographic controls × δ_t	✓	✓	✓	✓
Demographic controls × δ_t	✓	✓	✓	✓
Vulnerability controls × δ_t	✓	✓	✓	✓
Economic controls × δ_t	✓	✓	✓	✓
Observations	35 916	16 451	35 916	35 916
R^2	0.11	0.16	0.10	0.10

Notes: All of the specifications present OLS estimates and include month and municipality fixed effects. Standard errors clustered at the LLM level appear in parentheses. Significance values: ***p<0.01, **p<0.05, *p<0.10.

Table 4: Commuting indices and mortality growth (*red_zone*)

	mortality_growth			
	(1)	(2)	(3)	(4)
intensive_margin × *red_zone* × *February*	-0.143	-0.126	-0.115	-0.113
	(0.183)	(0.196)	(0.199)	(0.199)
intensive_margin × *red_zone* × *March*	0.950	0.634	0.762	0.774
	(0.618)	(0.621)	(0.610)	(0.604)
intensive_margin × *red_zone* × *April*	-0.577*	-0.525	-0.376	-0.366
	(0.323)	(0.326)	(0.332)	(0.334)
intensive_margin × *red_zone* × *May*	-0.498***	-0.463**	-0.442**	-0.439**
	(0.191)	(0.196)	(0.197)	(0.196)
extensive_margin × *red_zone* × *February*	1.571	0.728	0.478	0.481
	(1.867)	(1.899)	(1.928)	(1.929)
extensive_margin × *red_zone* × *March*	4.835	2.236	4.306	3.033
	(9.099)	(9.868)	(9.724)	(9.337)
extensive_margin × *red_zone* × *April*	3.054	2.190	3.598	3.206
	(2.892)	(3.133)	(2.838)	(2.736)
extensive_margin × *red_zone* × *May*	2.100	2.556	2.926	3.165
	(1.922)	(1.994)	(2.063)	(2.126)
intensive_margin × *February*	0.144	0.147	0.130	0.134
	(0.136)	(0.147)	(0.153)	(0.157)
intensive_margin × *March*	0.551***	0.757***	0.661***	0.764***
	(0.181)	(0.208)	(0.220)	(0.252)
intensive_margin × *April*	0.964***	0.939***	0.867***	0.923***
	(0.183)	(0.188)	(0.187)	(0.195)
intensive_margin × *May*	0.272**	0.234	0.244*	0.243
	(0.136)	(0.143)	(0.148)	(0.153)
extensive_margin × *February*	-3.171**	-1.518	-1.267	-1.365
	(1.544)	(1.772)	(1.815)	(1.832)
extensive_margin × *March*	-4.728*	-3.225	-5.602	-2.857
	(2.831)	(4.156)	(3.849)	(3.622)
extensive_margin × *April*	-1.700	-0.030	-2.787	-2.100
	(2.371)	(2.890)	(2.487)	(2.421)
extensive_margin × *May*	-1.992	-2.944	-3.814**	-4.488**
	(1.580)	(1.838)	(1.878)	(1.976)
red_zone × *February*	0.079	0.088	0.092	0.099
	(0.083)	(0.095)	(0.101)	(0.103)
red_zone × *March*	1.193***	1.425***	1.189***	1.144***
	(0.356)	(0.391)	(0.371)	(0.376)
red_zone × *April*	0.837***	0.823***	0.690***	0.691***
	(0.128)	(0.141)	(0.151)	(0.151)
red_zone × *May*	0.284***	0.265**	0.250**	0.271**
	(0.101)	(0.107)	(0.115)	(0.117)
constant	-0.033	-0.033	-0.033	-0.033
	(0.022)	(0.022)	(0.022)	(0.022)
Month FE	✓	✓	✓	✓
Municipality FE	✓	✓	✓	✓
Internal mobility × δ_t	✓	✓	✓	✓
Geographic controls × δ_t		✓	✓	✓
Demographic controls × δ_t		✓	✓	✓
Vulnerability controls × δ_t			✓	✓
Economic controls × δ_t				✓
Observations	35 916	35 916	35 916	35 916
R^2	0.12	0.12	0.12	0.13

Notes: All of the specifications present OLS estimates and include month and municipality fixed effects. Standard errors clustered at the LLM level appear in parentheses. Significance values: ***p<0.01, **p<0.05, *p<0.10.

Table 5: Commuting indices and mortality growth (*high_inactive*)

	mortality_growth		
	Italy	inside *red_zone*	outside *red_zone*
	(1)	(2)	(3)
intensive_margin × *high_inactive* × *February*	0.144	0.003	0.222
	(0.192)	(0.303)	(0.305)
intensive_margin × *high_inactive* × *March*	-0.084	0.202	-0.012
	(0.572)	(1.031)	(0.504)
intensive_margin × *high_inactive* × *April*	-0.651**	-0.457	-0.866**
	(0.296)	(0.547)	(0.342)
intensive_margin × *high_inactive* × *May*	-0.165	0.076	-0.318
	(0.198)	(0.345)	(0.301)
intensive_margin × *February*	0.045	0.055	0.092
	(0.126)	(0.202)	(0.183)
intensive_margin × *March*	1.391***	1.239**	0.733***
	(0.324)	(0.608)	(0.189)
intensive_margin × *April*	1.164***	0.826*	1.304***
	(0.241)	(0.488)	(0.247)
intensive_margin × *May*	0.167	-0.199	0.402**
	(0.139)	(0.229)	(0.188)
extensive_margin × *February*	-0.669	-0.861	-1.758
	(1.120)	(1.399)	(2.133)
extensive_margin × *March*	8.769	-0.491	-3.408
	(6.550)	(6.226)	(2.431)
extensive_margin × *April*	2.978*	-4.992**	-0.078
	(1.657)	(2.387)	(2.380)
extensive_margin × *May*	-1.765	-1.372	-4.751**
	(1.130)	(1.786)	(1.954)
high_inactive × *February*	-0.057	0.025	-0.095
	(0.086)	(0.158)	(0.117)
high_inactive × *March*	0.213	0.086	-0.027
	(0.248)	(0.557)	(0.191)
high_inactive × *April*	0.225**	0.242	0.177
	(0.113)	(0.266)	(0.138)
high_inactive × *May*	0.041	-0.005	0.034
	(0.091)	(0.196)	(0.119)
constant	-0.033	-0.035	-0.032**
	(0.024)	(0.053)	(0.015)
Month FE	✓	✓	✓
Municipality FE	✓	✓	✓
Internal mobility × δ_t	✓	✓	✓
Geographic controls × δ_t	✓	✓	✓
Demographic controls × δ_t	✓	✓	✓
Vulnerability controls × δ_t	✓	✓	✓
Economic controls × δ_t	✓	✓	✓
Observations	35 911	11 869	24 042
R^2	0.11	0.22	0.03

Notes: All of the specifications present OLS estimates and include month and municipality fixed effects. Standard errors clustered at the LLM level appear in parentheses. Significance values: ***p<0.01, **p<0.05, *p<0.10.

Supplemental File

Appendix A Additional Tables

Table A.1: Descriptive statistics

	Mean	SD	Minimum	Maximum	Observations
mortality_growth	0.313	1.540	-1.000	39.000	35916
intensive_margin	0.334	0.189	0.000	3.898	36725
extensive_margin	0.012	0.013	0.000	0.339	36725
internal_mobility	0.114	0.053	0.000	0.403	36725
coastal	0.078	0.268	0.000	1.000	36725
mountainous	0.732	0.443	0.000	1.000	36725
ln_density	4.718	1.406	-0.266	9.411	36725
ln_house_m^2*_pc*	3.763	0.134	3.266	4.450	36725
share_males	0.496	0.017	0.414	0.650	36725
*share_over*75	0.119	0.042	0.025	0.435	36725
*share_cohab_over*65	0.360	0.124	0.075	1.781	36725
hospital_beds_pc	0.004	0.001	0.000	0.007	36725
*pm*10	29.678	8.746	14.000	46.000	36725
district	0.265	0.441	0.000	1.000	36725
remote_working	0.471	0.019	0.384	0.609	36725

Notes: The table reports standard descriptive statistics of the variables used in the empirical analysis.

Table A.2: Variables description

Variable	Measure	Year[a]	Unit of observation	Source
mortality_growth	Growth rate between the 2020 monthly fatalities and the 2015-2019 average monthly fatalities.	2020	Municipality	ISTAT
intensive_margin	Sum of out-flows and in-flows divided by total population.	2011	Municipality	ISTAT
extensive_margin	Sum of outward and inward connections divided by maximum possible number of connections.	2011	Municipality	ISTAT
internal_mobility	Self-flows divided by total population.	2011	Municipality	ISTAT
coastal	Dummy equal to 1 if the municipality is located near the sea.	2011	Municipality	ISTAT
mountainous	Dummy equal to 1 if the municipality is located at medium-high altitude.	2011	Municipality	ISTAT
ln_density	Log of population divided by municipality area (km^2).	2019	Municipality	ISTAT
ln_house_m2_pc	Log of the average number of m^2 per inhabitant.	2011	Municipality	ISTAT
share_males	Male population divided by total population.	2019	Municipality	ISTAT
share_over75	Population older than 75 years old divided by total population.	2011	Municipality	ISTAT
share_cohab_over65	Number of individuals older than 65 years old divided by total cohabitants.	2011	Municipality	ISTAT
hospital_beds_pc	Number of hospital beds per inhabitant.	2017	Province	ISTAT
pm10	Average value of $\mu g/m^3$.	2017	Province	ISPRA
district	Dummy equal to 1 if the municipality is located within an industrial district.	2011	Municipality	ISTAT
remote_working	Weighted average of the labour force composition for the 1-digit ATECO working remotely indices.	2011	Municipality	ISTAT

[a] Note that the number of Italian municipalities decreased from 8 092 in 2011 to 7 904 in 2020. Hence, we precisely combined data by considering all of the administrative variations occurring in Italy during these 9 years, such as the establishment of new municipalities and the suppression of others. Considering that *mortality_growth* data are available for 7 357 municipalities, we ended up with 7 345 observations for each month.

Table A.3: Commuting indices and mortality growth (part 3)

	mortality_growth			
	(1)	(2)	(3)	(4)
intensive_margin × *February*	0.114	0.120	0.096	0.098
	(0.095)	(0.102)	(0.103)	(0.108)
intensive_margin × *March*	1.896***	1.804***	1.430***	1.427***
	(0.299)	(0.292)	(0.285)	(0.277)
intensive_margin × *April*	1.141***	1.034***	0.882***	0.906***
	(0.170)	(0.173)	(0.166)	(0.162)
intensive_margin × *May*	0.153	0.107	0.095	0.095
	(0.094)	(0.099)	(0.104)	(0.108)
extensive_margin × *February*	-1.881**	-0.698	-0.748	-0.771
	(0.891)	(1.075)	(1.086)	(1.093)
extensive_margin × *March*	14.000	11.820	6.064	8.556
	(8.531)	(7.995)	(6.930)	(6.596)
extensive_margin × *April*	6.032***	6.263***	2.643*	3.442**
	(1.767)	(1.680)	(1.567)	(1.590)
extensive_margin × *May*	0.198	-0.405	-1.352	-1.620
	(0.926)	(1.026)	(1.054)	(1.109)
internal_mobility × *February*	0.412	0.406	0.472	0.484
	(0.318)	(0.342)	(0.346)	(0.367)
internal_mobility × *March*	-2.033	-1.700	-0.042	-0.483
	(1.299)	(1.288)	(1.129)	(1.206)
internal_mobility × *April*	-0.584	-0.205	0.473	0.396
	(0.513)	(0.506)	(0.520)	(0.531)
internal_mobility × *May*	-0.049	0.154	0.215	0.265
	(0.349)	(0.357)	(0.361)	(0.381)
coastal × *February*		-0.065	-0.060	-0.062
		(0.047)	(0.049)	(0.051)
coastal × *March*		-0.398***	-0.215**	-0.182**
		(0.106)	(0.100)	(0.091)
coastal × *April*		-0.228***	-0.155**	-0.157**
		(0.063)	(0.065)	(0.073)
coastal × *May*		-0.085*	-0.061	-0.064
		(0.048)	(0.049)	(0.051)
mountainous × *February*		0.027	0.028	0.027
		(0.034)	(0.037)	(0.037)
mountainous × *March*		-0.281	-0.073	-0.073
		(0.177)	(0.167)	(0.167)
mountainous × *April*		-0.064	-0.002	-0.005
		(0.080)	(0.076)	(0.076)
mountainous × *May*		0.046	0.051	0.0513
		(0.040)	(0.044)	(0.043)
ln_density × *February*		-0.014	0.003	0.004
		(0.020)	(0.022)	(0.022)
ln_density × *March*		-0.035	-0.056	-0.057
		(0.059)	(0.066)	(0.060)
ln_density × *April*		-0.001	-0.018	-0.014
		(0.030)	(0.035)	(0.038)
ln_density × *May*		0.026	0.018	0.018
		(0.020)	(0.021)	(0.022)
ln_house_m^2*_pc* × *February*		-0.018	0.007	0.011
		(0.149)	(0.169)	(0.171)
ln_house_m^2*_pc* × *March*		-0.636	-1.428**	-1.561***
		(0.490)	(0.581)	(0.572)
ln_house_m^2*_pc* × *April*		0.476*	-0.063	-0.082
		(0.243)	(0.291)	(0.299)
ln_house_m^2*_pc* × *May*		0.239	0.087	0.010

Continued on next page

Table A.3 – continued from previous page

	mortality_growth			
	(1)	(2)	(3)	(4)
		(0.183)	(0.196)	(0.202)
$share\_males \times February$			2.425	2.420
			(1.631)	(1.649)
$share\_males \times March$			8.683***	7.528***
			(2.969)	(2.621)
$share\_males \times April$			-1.242	-1.605
			(1.888)	(1.851)
$share\_males \times May$			-2.777*	-2.658*
			(1.480)	(1.479)
$share\_over75 \times February$			0.361	0.385
			(1.855)	(1.879)
$share\_over75 \times March$			-0.789	-0.301
			(3.609)	(3.533)
$share\_over75 \times April$			-3.932	-3.759
			(2.607)	(2.595)
$share\_over75 \times May$			0.396	0.306
			(1.944)	(1.952)
$share\_cohab\_over65 \times February$			-0.058	-0.070
			(0.673)	(0.680)
$share\_cohab\_over65 \times March$			0.531	0.485
			(1.195)	(1.181)
$share\_cohab\_over65 \times April$			1.737*	1.714*
			(0.949)	(0.950)
$share\_cohab\_over65 \times May$			0.006	0.016
			(0.709)	(0.717)
$hospital\_beds\_pc \times February$			20.600	20.320
			(21.620)	(21.680)
$hospital\_beds\_pc \times March$			-43.860	-44.200
			(64.560)	(66.320)
$hospital\_beds\_pc \times April$			60.520**	60.000**
			(30.090)	(30.230)
$hospital\_beds\_pc \times May$			31.110	30.830
			(24.050)	(24.130)
$pm10 \times February$			-0.001	-0.001
			(0.003)	(0.003)
$pm10 \times March$			0.054***	0.049***
			(0.012)	(0.011)
$pm10 \times April$			0.022***	0.021***
			(0.005)	(0.005)
$pm10 \times May$			0.005*	0.005*
			(0.003)	(0.003)
$district \times February$				-0.010
				(0.045)
$district \times March$				0.531*
				(0.280)
$district \times April$				0.133
				(0.093)
$district \times May$				-0.053
				(0.049)
$remote\_working \times February$				-0.038
				(1.339)
$remote\_working \times March$				-8.424***
				(2.750)
$remote\_working \times April$				-3.301*
				(1.959)
$remote\_working \times May$				0.876

Continued on next page

Table A.3 – continued from previous page

	mortality_growth			
	(1)	(2)	(3)	(4)
				(1.370)
constant	-0.034	-0.034	-0.034	-0.033
	(0.025)	(0.025)	(0.024)	(0.024)
Month FE	✓	✓	✓	✓
Municipality FE	✓	✓	✓	✓
Observations	35 916	35 916	35 916	35 916
R^2	0.08	0.09	0.10	0.11

Notes: All of the specifications present OLS estimates and include month and municipality fixed effects. Standard errors clustered at the LLM level appear in parentheses. Significance values: ***p<0.01, **p<0.05, *p<0.10. Almost all coefficients associated with the control variables respect the expected sign during the most critical part of the pandemic cycle (i.e., March and April). Among those statistically significant, excess mortality appears to be - *ceteris paribus* - higher in municipalities with a larger share of males, with more intergenerational dependence, with more hospital beds per inhabitant, with higher pollution levels, and with a denser local labour market. On the other hand, excess mortality seems to be lower in municipalities with a plausibly better air quality (i.e., near the sea) and with larger numbers of potential "remote" workers.

Table A.4: ATECO sectors allowed to operate during the "economic" lockdown

ATECO		Description
Section	Code	
A: Agriculture	01	Crop and animal production
	03	Fishing and aquaculture
B: Mining	05	Mining of coal and lignite
	06	Extraction of crude petroleum and natural gas
	09.1	Support activities for petroleum and natural gas extraction
C: Manufacturing	10	Manufacture of food products
	11	Manufacture of beverages
	13.95	Manufacture of non-wovens and articles made from non-wovens, except apparel
	13.96	Manufacture of other technical and industrial textiles
	14.12	Manufacture of workwear
	16.24	Manufacture of wooden containers
	17	Manufacture of paper and paper products
	18	Printing and reproduction of recorded media
	19	Manufacture of coke and refined petroleum products
	20	Manufacture of chemicals and chemical products
	21	Manufacture of basic pharmaceutical products and pharmaceutical preparations
	22.2	Manufacture of plastic products
	23.13	Manufacture of hollow glass
	23.19	Manufacture and processing of other glass, including technical glassware
	25.21	Manufacture of central heating radiators and boilers
	25.92	Manufacture of light metal packaging
	26.6	Manufacture of irradiation, electromedical and electrotherapeutic equipment
	27.1	Manufacture of electric motors, generators, transformers and electricity distribution
	27.2	Manufacture of batteries and accumulators
	28.29	Manufacture of other general-purpose machinery n.e.c.[a]
	28.95	Manufacture of machinery for paper and paperboard production
	28.96	Manufacture of plastic and rubber machinery
	32.50	Manufacture of medical and dental instruments and supplies
	32.99	Other manufacturing n.e.c.[a]
	33	Repair and installation of machinery and equipment
D: Energy, Gas	35	Electricity, gas, steam and air conditioning supply
E: Water, Waste	36	Water collection, treatment and supply
	37	Sewerage
	38	Waste collection, treatment and disposal activities; materials recovery
	39	Remediation activities and other waste management services
F: Construction	42	Civil engineering
	43.2	Electrical, plumbing and other construction installation activities
G: Trade	45.2	Maintenance and repair of motor vehicles
	45.3	Sale of motor vehicle parts and accessories
	45.4	Sale, maintenance and repair of motorcycles and related parts and accessories
	46.2	Wholesale of agricultural raw materials and live animals

Continued on next page

Table A.4 – continued from previous page

ATECO		Description
Section	Code	
	46.3	Wholesale of food, beverages and tobacco
	46.46	Wholesale of pharmaceutical goods
	46.49	Wholesale of other household goods
	46.61	Wholesale of agricultural machinery, equipment and supplies
	46.69	Wholesale of other machinery and equipment
	46.71	Wholesale of solid, liquid and gaseous fuels and related products
H: Transportation	49	Land transport and transport via pipelines
	50	Water transport
	51	Air transport
	52	Warehousing and support activities for transportation
	53	Postal and courier activities
I: Accommodation	55.1	Hotels and similar accommodations
J: Information	58	Publishing activities
	59	Motion picture, video and television programme production and sound recording
	60	Programming and broadcasting activities
	61	Telecommunications
	62	Computer programming, consultancy and related activities
	63	Information service activities
K: Finance, Insurance	64	Financial service activities, except insurance and pension funding
	65	Insurance, reinsurance and pension funding, except compulsory social security
	66	Activities auxiliary to financial services and insurance activities
M: Professional services	69	Legal and accounting activities
	70	Activities of head offices; management consultancy activities
	71	Architectural and engineering activities; technical testing and analysis
	72	Scientific research and development
	74	Other professional, scientific and technical activities
	75	Veterinary activities
N: Other services	78.2	Temporary employment agency activities
	80.1	Private security activities
	80.2	Security systems service activities
	81.2	Cleaning activities
	82.20	Activities of call centres
	82.92	Packaging activities
	82.99	Other business support service activities n.e.c.[a]
O: Public administration	84	Public administration and defence; compulsory social security
P: Education	85	Education
Q: Health	86	Human health activities
	87	Residential care activities
	88	Social work activities without accommodations
S: Other activities	94	Activities of membership organizations
	95.11	Repair of computers and peripheral equipment

Continued on next page

Table A.4 – continued from previous page

ATECO		Description
Section	Code	
	95.12	Repair of communication equipment
	95.22	Repair of household appliances and home and garden equipment
T: Household activities	97	Activities of households as employers of domestic personnel

[a] Not elsewhere classified.

Notes: We refer to the revised list of ATECO sectors provided by the Italian government on March 25, which integrated the previous list provided on March 22. Some of the ATECO categories are specified also at the 5-digit level. For simplicity, we consider as active any 4-digit ATECO sector embedding the 5-digit one.

Appendix B Additional Figures

Figure B.1: Evolution of *mortality_growth* in Italy, January-May 2020

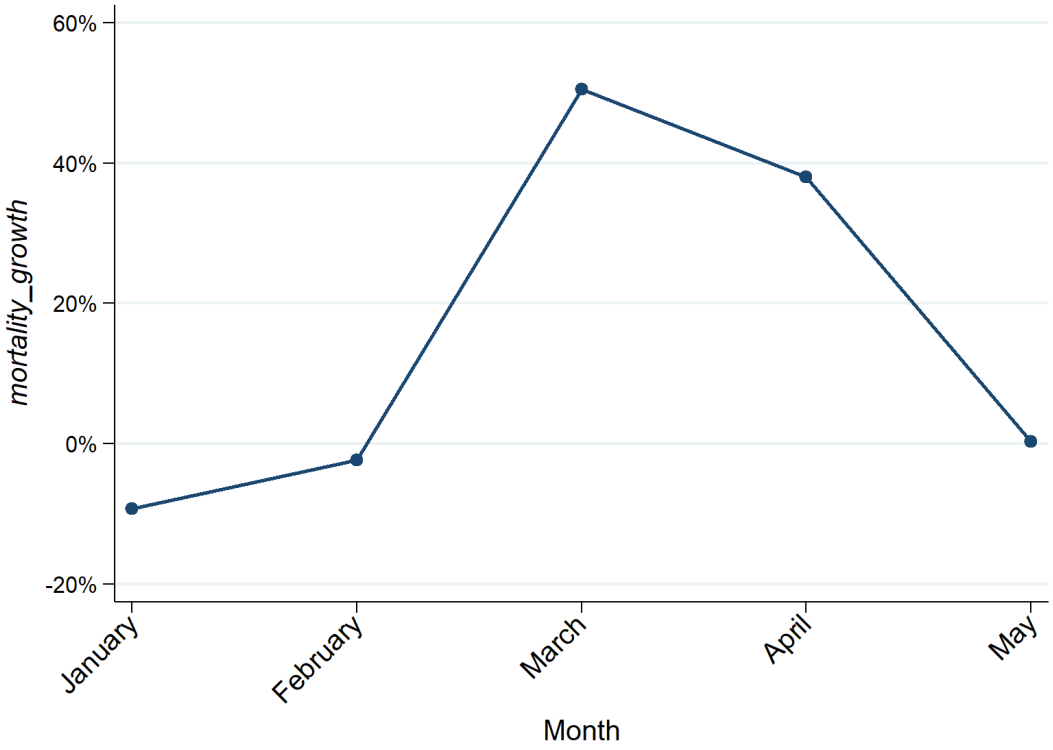

Notes: The figure plots the evolution of excess mortality in Italy during the period of analysis. It points out how the containment measures adopted in March 2020 were essential in flattening the curve since *mortality_growth* was reduced to almost the pre-pandemic level by May. *Source*: Authors' own elaboration.

Figure B.2: Correlation matrix among explanatory variables

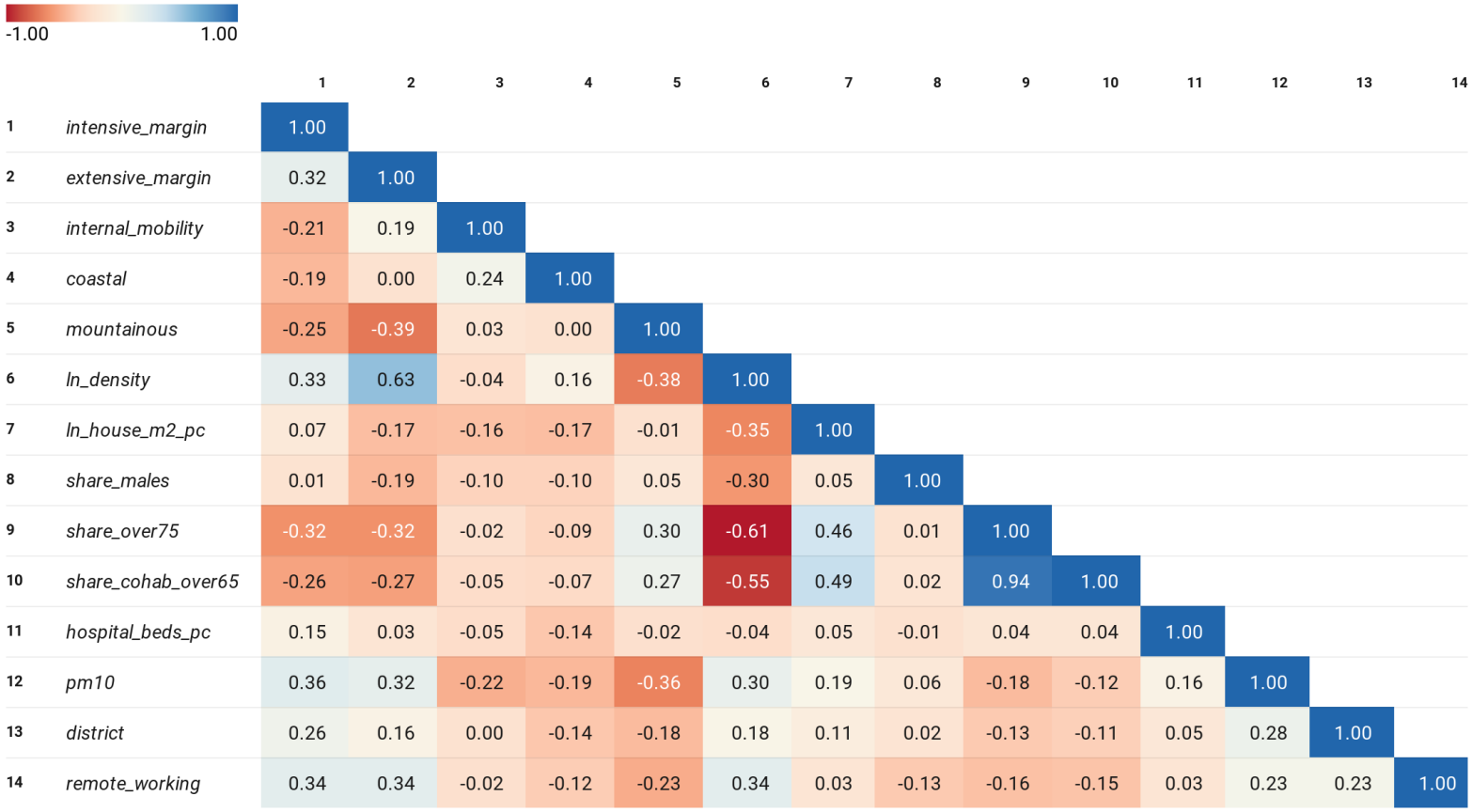

Notes: The figure reports a correlation matrix among explanatory variables used in the empirical analysis. *Source*: Authors' own elaboration.

Figure B.3: *mortality_growth*, by month and municipality

(a) January 2020

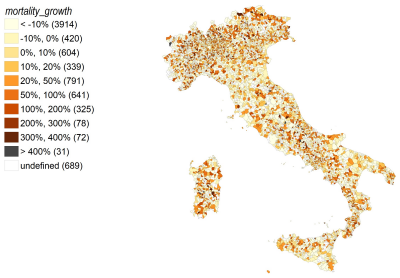

(b) February 2020

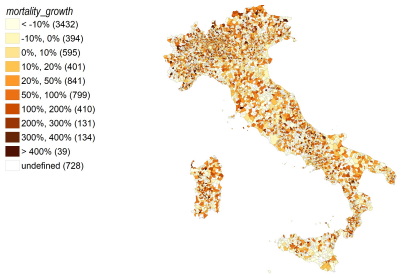

(c) March 2020

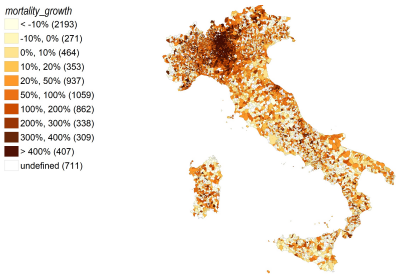

(d) April 2020

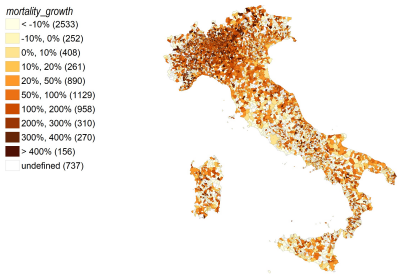

(e) May 2020

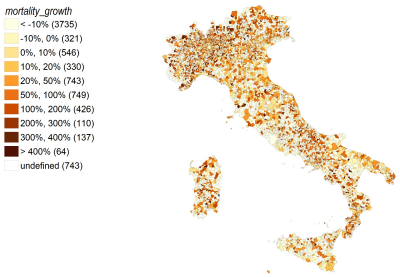

Source: Authors' own elaboration.

Figure B.4: Control variables, by municipality

(a) *internal_mobility*

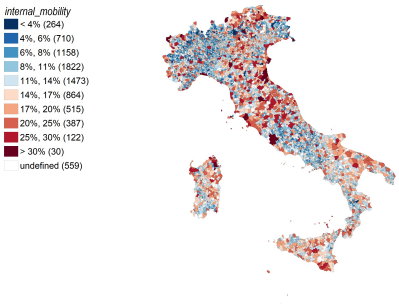

(b) *share_over75*

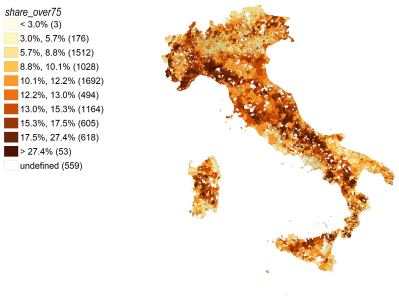

(c) *hospital_beds_pc*

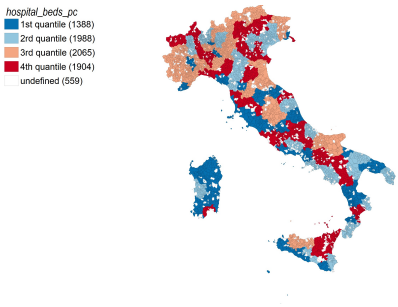

(d) *pm10*

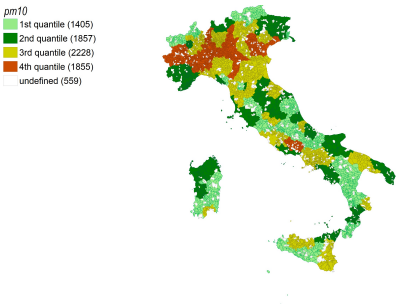

(e) *district*

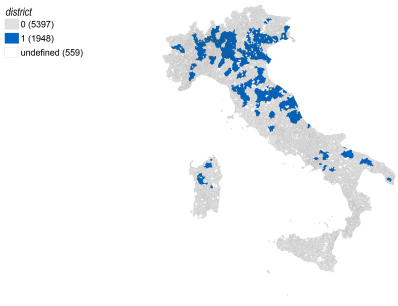

(f) *remote_working*

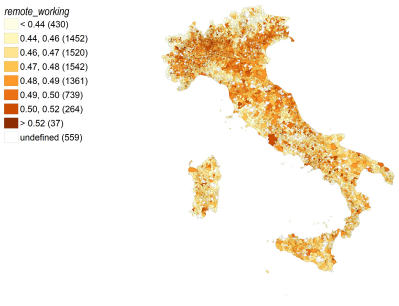

Source: Authors' own elaboration.

Figure B.5: Estimated coefficients of the commuting indices, by month

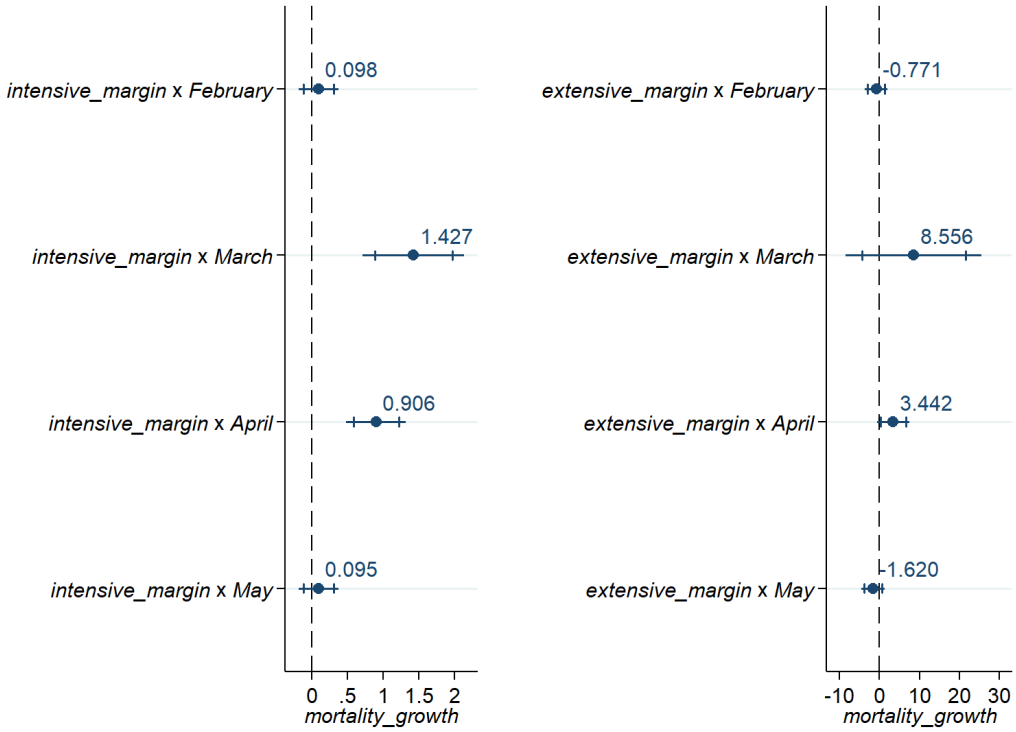

Notes: The figure plots the coefficients of the specification in column 4 of Table 2. Horizontal bands represent ± 1.96 and ± 2.58 times the standard error of each point estimate. The figure clearly shows the decreasing trend over time in the magnitude of all coefficients from March onwards, suggesting how the lockdown was crucial in reducing excess mortality. *Source*: Authors' own elaboration.

Figure B.6: Relationship between the 2011 and 2019 shares of outgoing flows

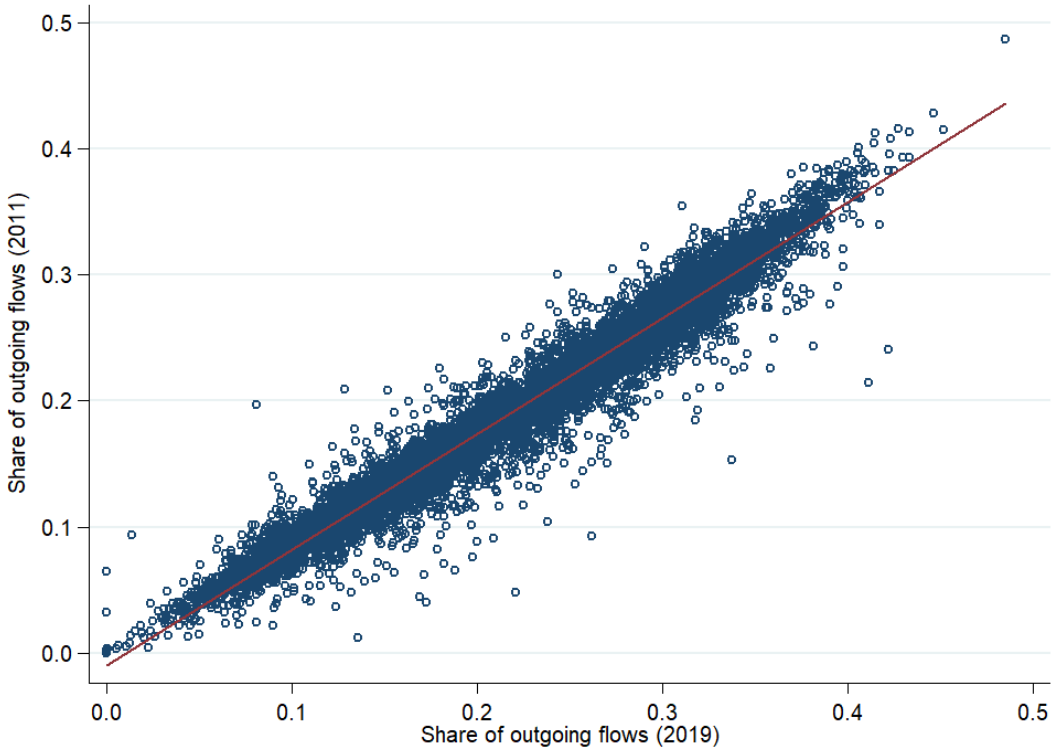

Notes: The figure plots the 2011 and 2019 shares of outgoing flows, indicating the total number of workers moving from a municipality over the corresponding-year population. The figure clearly shows an almost one-to-one association between the two shares ($R^2 = 0.95$), suggesting how the spatial patterns of work-related mobility is remarkably preserved over time. *Source*: Authors' own elaboration.